Published for SISSA by Springer

Received: *June 11, 2010*
Accepted: *July 19, 2010*
Published: *August 6, 2010*

Holographic studies of quasi-topological gravity

Robert C. Myers,[a] **Miguel F. Paulos**[b] **and Aninda Sinha**[a]

[a] *Perimeter Institute for Theoretical Physics, Waterloo, Ontario N2L 2Y5, Canada*
[b] *Department of Applied Mathematics and Theoretical Physics, Cambridge CB3 0WA, U.K.*

E-mail: rmyers@perimeterinstitute.ca, asinha@perimeterinstitute.ca, m.f.paulos@damtp.cam.ac.uk

Abstract: Quasi-topological gravity is a new gravitational theory including curvature-cubed interactions and for which exact black hole solutions were constructed. In a holographic framework, classical quasi-topological gravity can be thought to be dual to the large N_c limit of some non-supersymmetric but conformal gauge theory. We establish various elements of the AdS/CFT dictionary for this duality. This allows us to infer physical constraints on the couplings in the gravitational theory. Further we use holography to investigate hydrodynamic aspects of the dual gauge theory. In particular, we find that the minimum value of the shear-viscosity-to-entropy-density ratio for this model is $\eta/s \simeq 0.4140/(4\pi)$.

Keywords: Gauge-gravity correspondence, AdS-CFT Correspondence, Black Holes in String Theory

ArXiv ePrint: 1004.2055

doi:10.1007/JHEP08(2010)035

JHEP08(2010)035

Contents

JHEP08(2010)035

1 Introduction

The AdS/CFT correspondence has proven a fertile ground for investigating the properties of strongly coupled gauge theories [1, 2], in particular the thermodynamic and hydrodynamic properties of these gauge theories at finite temperature [3–5]. However, such investigations face acute limitations because at present, we have an insufficient understanding of string theory in interesting holographic backgrounds, i.e., in spacetimes with Ramond-Ramond fields. Hence the examination of holographic gauge theories is primarily confined to both the limit of a large 't Hooft coupling λ and a large number of colours N_c where the dual gravitational theory corresponds to (semi-)classical Einstein gravity with a two-derivative bulk action. However, it is understood that accounting for higher curvature interactions, or higher derivative interactions more generally, within a perturbative framework allows one

to begin to consider finite λ and finite N_c corrections [6–12]. An alternative point of view would be that admitting such higher curvature (or higher derivative) interactions introduces new couplings amongst the operators in the dual CFT, thereby broadening the universality class of dual CFT's which one can study with holography [11–14]. If one examines a point in the space of CFT's where these new couplings are finite, the higher curvature terms will now make finite contributions in the analysis of the dual gravity theory. However, if any higher curvature term were to become important, the normal expectation is that an infinite number of such terms will become important at the same time as the background curvature must have reached the string or Planck scales. The relevance of all these terms is really signalling that one has entered a regime where the dual gravitational theory cannot be described by a local quantum field theory. Hence to properly investigate the effects of these finite CFT couplings, one is brought back to the question of understanding string theory in interesting holographic backgrounds.

However, a traditional avenue to progress in theoretical physics is the study of simplified or toy models which might provide insight into the behaviour of some complex physical system of interest. Recent work with Gauss-Bonnet (GB) gravity showed that the utility of such toy models in a holographic framework [15–18, 20, 21]. In this case, the usual Einstein action is supplemented by a certain curvature-squared interaction, which corresponds precisely to the four-dimensional Euler density. With this extension of the usual Einstein action in the five-dimensional bulk gravity theory, the class of holographic models is extended to allow independent values of the two central charges a and c of the dual CFT [24–26]. Further it was found that GB gravity still captures certain fundamental constraints which can also be inferred from direct considerations of CFT's alone. In particular, consistency of the CFT constrains the central charges to obey [13]: $1/2 \leq a/c \leq 3/2$. Hence GB gravity (or more generally Lovelock gravity in higher dimensions [27–30]) provides an interesting toy model to examine questions related to holographic hydrodynamics, or perhaps the holographic c-theorem [31, 32].

Motivated by the success of holographic studies of GB gravity, this holographic model was recently extended with the introduction of a new curvature-cubed interaction in quasi-topological gravity [36]. The progress with GB gravity relies on the fact that even though this is a higher curvature theory of gravity, the holographic calculations in this model are still under control. This control stems from two properties of the theory: the equations of motion are only second order in derivatives and exact black hole solutions have been constructed. In quasi-topological gravity, exact black hole solutions are again readily constructed but on general backgrounds the equations of motion will be fourth order in derivatives [36]. Remarkably, however, the linearized equations of motion in an AdS_5 background are again second order and in fact, match precisely the linearized equations of the Einstein theory [36]. As we will show in the following, these properties are sufficient to allow us to examine many interesting features of the holographic framework established by this new toy model. The new curvature-cubed interactions again expand the class of CFT's which can be realized with this model. In particular, the new couplings are generalized such that the dual CFT will not be supersymmetric [13] and so this holographic model may provide new insights on non-supersymmetric gauge theories with a conformal fixed point.

One aspect which we examine with this new holographic model are the hydrodynamic

JHEP08(2010)035

transport coefficients of the dual CFT, in particular the shear viscosity. It has been observed that the ratio of shear viscosity to density entropy of typical holographic fluids is extremely small in comparison to typical fluids for ordinary matter [3, 4]. Originally it was conjectured that these holographic calculations provided a universal lower bound, namely $\eta/s \geq 1/4\pi$. One piece of circumstantial evidence for this conjecture came from string theory were it was found that the leading finite λ corrections always raised η/s above the bound for supersymmetric plasmas where $c = a$ [6, 7, 9, 10]. However, it is now understood this KSS bound can be violated in string theory duals of plasmas where $c \neq a$ by the effect of new curvature-squared interactions in the gravitational action [8, 11, 12]. However, the string theory constructions where these higher curvature terms are under control only allow for small perturbative violations of the KSS bound. General arguments still suggest that the ratio of the shear viscosity to entropy density should satisfy some lower bound [3, 4, 37] and so the question naturally arises as to the precise nature of such a bound. Hence it is certainly of interest to explore situations where finite violations of the bound occur and the toy models above provide a framework for such explorations. In particular, it would be interesting if one was able to show that η/s could be pushed to zero without producing any other pathologies developing in the theory. With quasi-topological gravity, we find that η/s reaches a non-zero lower value in a particular corner of the allowed space of gravitational couplings.

An outline of the rest of the paper is as follows: In section 2, we present a brief review of quasi-topological gravity in five dimensions and the black hole solutions of the theory. We begin to establish the AdS/CFT dictionary for this gravitational theory in section 3 with a calculation of the central charges of the dual CFT. In section 4, we adapt the scattering experiments in the CFT of [13] to a holographic calculation. These computations yield directly the flux coefficients t_2 and t_4, but combined with the expressions for the central charges, we are also able to express the coefficients $\mathcal{A}$, $\mathcal{B}$ and $\mathcal{C}$, which determine the three-point functions of the stress tensor, in terms of the gravitational couplings. Next in section 5, we consider various constraints on the gravitational couplings which are required to ensure the physical consistency of the dual CFT. We consider three independent constraints: positivity of the central charge c, positivity of the energy fluxes in section 4 and avoiding violations of causality. In section 6, we examine the hydrodynamic behaviour of the CFT plasma. In particular, we find that the minimum value of the ratio of the shear viscosity to the entropy density in this model is $\eta/s \simeq 0.4140/(4\pi)$. We provide a preliminary analysis of possible instabilities of the black holes, or alternatively of a uniform plasma in the dual CFT at finite temperature in section 7. We conclude with a brief discussion of our results and future directions in section 8.

2 Review of quasi-topological gravity

We begin with a review of some salient features of quasi-topological gravity. We focus on the five-dimensional version of the gravity theory, which would be dual to a four-dimensional CFT. The bulk gravity action can be written as [36]:

$$I = \frac{1}{2\ell_{\rm P}^3}\int d^5x\sqrt{-g}\left[\frac{12}{L^2} + R + \frac{\lambda}{2}L^2\mathcal{X}_4 + \frac{7}{8}\mu L^4\mathcal{Z}_5'\right] \tag{2.1}$$

JHEP08(2010)035

where $\mathcal{X}_4$ is the four-dimensional Euler density, as used in GB gravity

$$\mathcal{X}_4 = R_{\mu\nu\rho\sigma}R^{\mu\nu\rho\sigma} - 4\,R_{\mu\nu}R^{\mu\nu} + R^2\,, \tag{2.2}$$

and $\mathcal{Z}_5'$ is the new curvature-cubed interaction

$$\begin{aligned}\mathcal{Z}_5' = {} & R_{\mu\nu}{}^{\rho\sigma}R_{\rho\sigma}{}^{\alpha\beta}R_{\alpha\beta}{}^{\mu\nu} + \frac{1}{14}\,(21\,R_{\mu\nu\rho\sigma}R^{\mu\nu\rho\sigma}R - 120\,R_{\mu\nu\rho\sigma}R^{\mu\nu\rho}{}_{\alpha}R^{\sigma\alpha} \\ & +144\,R_{\mu\nu\rho\sigma}R^{\mu\rho}R^{\nu\sigma} + 128\,R_{\mu}{}^{\nu}R_{\nu}{}^{\rho}R_{\rho}{}^{\mu} - 108\,R_{\mu}{}^{\nu}R_{\nu}{}^{\mu}R + 11\,R^3)\ .\end{aligned} \tag{2.3}$$

The AdS vacua of this theory have a curvature scale given by

$$\frac{1}{\tilde{L}^2} = \frac{f_\infty}{L^2} \tag{2.4}$$

where the constant f_∞ is determined as one of the roots of

$$1 - f_\infty + \lambda f_\infty^2 + \mu f_\infty^3 = 0\ . \tag{2.5}$$

Note for any choice of the couplings λ and μ, there is at most one ghost-free AdS vacuum which supports nonsingular black hole solutions, as described in detail in [36]. The solutions describing planar AdS black holes take the form

$$\mathrm{d}s^2 = \frac{r^2}{L^2}\left(-\frac{f(r)}{f_\infty}\,\mathrm{d}t^2 + \mathrm{d}x_1^2 + \mathrm{d}x_2^2 + \mathrm{d}x_3^2\right) + \frac{L^2}{r^2 f(r)}\,\mathrm{d}r^2\,, \tag{2.6}$$

where $f(r)$ is determined by roots of the following cubic equation:

$$1 - f(r) + \lambda f(r)^2 + \mu f(r)^3 = \frac{r_0^4}{r^4}\ . \tag{2.7}$$

For the relevant solutions, the black hole horizon occurs at $r = r_0$, which is easily seen to yield $f(r = r_0) = 0$ as a solution of the above equation. The Hawking temperature is given by

$$T = \frac{r_0}{\pi L^2}\frac{1}{f_\infty^{1/2}}\ . \tag{2.8}$$

The energy and entropy densities are simply calculated as [36]:

$$\rho = \frac{3r_0^4}{2\ell_{\rm P}^3 L^5 f_\infty^{1/2}}\,, \qquad\qquad s = \frac{2\pi r_0^3}{\ell_{\rm P}^3 L^3}\ . \tag{2.9}$$

Further note that these relations satisfy $\rho = \frac{3}{4}Ts$, as expected for a four-dimensional CFT (in the absence of a chemical potential).

Apart from finding exact black hole solutions, another remarkable property of quasi-topological gravity is that the linearized graviton equations in the five-dimensional AdS vacuum take the form [36]:

$$\begin{aligned}-\frac{1}{2}\,(1 - 2\lambda f_\infty - 3\mu f_\infty^2)\,\Big[& \nabla^2 h_{ab} + \nabla_a\nabla_b\,h_c{}^c - \nabla_a\nabla^c h_{cb} - \nabla_b\nabla^c h_{ca} \\ & - g_{ab}^{[0]}\left(\nabla^2 h_c{}^c - \nabla^c\,\nabla^d h_{cd}\right) + \frac{2}{\tilde{L}^2}\,h_{ab} - \frac{2}{\tilde{L}^2}\,g_{ab}^{[0]}\,h_c{}^c\Big] = \ell_{\rm P}^3\,\hat{T}_{ab}\,.\end{aligned} \tag{2.10}$$

JHEP08(2010)035

Here $g^{[0]}_{ab}$ is the background AdS_5 metric and $\tilde{L}$ is the curvature scale in eq. (2.4). Hence the observation is that in the AdS_5 background, the linearized equations are only second order in derivatives. In fact, up to an overall factor, the above equations (2.10) are precisely the same as the linearized equations for Einstein gravity in an AdS_5 background — for example, see [38, 39]. This result contrasts with that for a generic R^3 action which would yield fourth order equations of motion.[1] However, the same occurs here for quasi-topological gravity on a general spacetime geometry. That is, on general backgrounds, the linearized equations are fourth order in derivatives for the present theory as well.

3 Central charges

In this section and the following section, we develop the dictionary relating the couplings in five-dimensional quasi-topological gravity to parameters which characterize the dual four-dimensional CFT. Since we are only dealing with the gravitational sector of the AdS theory, we are looking to examine the behaviour of the stress energy tensor of the CFT. Two such parameters are the central charges, c and a, of the CFT. We calculate these through their appearance in the trace anomaly [24], using the now standard holographic approach of [44, 45]. The central charge c also fixes the coefficient of the leading singularity in the operator product of the stress tensor with itself [46–50]. Hence as a verification of our first calculation, we also determine c from examining the two-point function in section 3.2.

3.1 Holographic trace anomaly

The two central charges of a four-dimensional CFT can be defined by the trace anomaly that arises when the CFT is placed on a curved background geometry [24]:

$$\langle\, T_a{}^a \,\rangle = \frac{c}{16\pi^2}\, I_4 - \frac{a}{16\pi^2}\, \mathcal{X}_4\,, \tag{3.1}$$

where $\mathcal{X}_4$ is the four-dimensional Euler density, whose structure is given in eq. (2.2) (although here, $\mathcal{X}_4$ is evaluated for the four-dimensional background metric of the CFT), and I_4 is the square of the Weyl tensor, i.e.,

$$I_4 = C_{abcd}\, C^{abcd} = R_{abcd}\, R^{abcd} - 2\, R_{ab} R^{ab} + \frac{1}{3}\, R^2\,, \tag{3.2}$$

In order to compute c and a for the CFT dual to quasi-topological gravity, we follow the holographic procedure described in [44, 45]. We should note that modifications to the central charges from R^2 interactions were examined previously in [25, 26] while perturbative corrections coming from R^3 interactions were considered in [51]. Efficient methods, i.e., 'short cuts' to calculate the holographic trace anomalies for an arbitrary gravitational action are discussed in [32–35].

Following [44, 45], we begin with the Fefferman-Graham expansion

$$\mathrm{d}s^2 = \frac{\tilde{L}^2}{4\rho^2}\mathrm{d}\rho^2 + \frac{g_{ab}}{\rho}\,\mathrm{d}x^a \mathrm{d}x^b\,, \tag{3.3}$$

[1] Recently, other theories of curvature-cubed gravity with exceptional properties were identified in [40–43]. In fact, up to a contribution proportional to the six-dimensional Euler density, the curvature-cubed interaction constructed in five dimensions by [42, 43] is identical to that studied here.

JHEP08(2010)035

with

$$g_{ab} = g_{(0)ab} + \rho\, g_{(1)ab} + \rho^2 g_{(2)ab} + \cdots\,, \tag{3.4}$$

where the boundary metric $g_{(0)ab}$ corresponds to the background geometry of the dual CFT. The next step is to substitute this expansion of the metric into the gravity action (2.1). On-shell $g_{(2)}$ drops out and we are left with an action involving $g_{(0)}$ and $g_{(1)}$. To extract the conformal anomaly, we focus on terms which when integrated produce a log divergence. This leads to

$$\begin{aligned} I = \mathcal{N} \int_\epsilon \frac{d\rho}{\rho} \int d^4x \sqrt{g_{(0)}} \Big[\Big(t_1\, R^{(0)^2} + t_2\, R^{(0)}_{ab} R^{(0)ab} + t_3\, R^{(0)}_{abcd}\, R^{(0)abcd} \Big) \\ + A\, R^{(0)ab} g_{(1)ab} + B\, R^{(0)}\, \mathrm{tr}\, g_{(1)} + C\, \mathrm{tr}\, g_{(1)}^2 + D\, (\mathrm{tr}\, g_{(1)})^2 \Big]\,. \end{aligned} \tag{3.5}$$

where, e.g., $R^{(0)}_{ab}$ corresponds to the Ricci tensor calculated for the boundary metric $g_{(0)ab}$. Further ϵ defines a UV regulator surface which cuts off the radial integral. The constant coefficients appearing in the above expression (3.5) are given by

$$\begin{aligned} t_1 &= \frac{1}{2}(\lambda f_\infty - 3\mu f_\infty^2) = -4t_2 = t_3\,, \\ A &= -(1 - 2\lambda f_\infty - 3\mu f_\infty^2) = -2\,B = C\,, \\ D &= -\frac{1}{6}(7 - \lambda f_\infty + 5\mu f_\infty^2)\,, \quad \mathcal{N} = \frac{L^3}{\ell_{\rm P}^3 f_\infty^{3/2}}\,. \end{aligned} \tag{3.6}$$

Next we eliminate $g_{(1)ij}$ using its equation of motion and then following [44, 45], we can interpret the result as

$$I \simeq -\log\epsilon\, \frac{1}{2} \int d^4x \sqrt{g_{(0)}}\, \langle\, T_a{}^a \,\rangle\,. \tag{3.7}$$

Hence comparing the coefficients of the various terms involving the background curvatures with eq. (3.1), we find

$$c = \pi^2 \frac{L^3}{\ell_{\rm P}^3} \frac{1}{f_\infty^{3/2}} \left(1 - 2\lambda f_\infty - 3\mu f_\infty^2\right)\,, \tag{3.8}$$

$$a = \pi^2 \frac{L^3}{\ell_{\rm P}^3} \frac{1}{f_\infty^{3/2}} \left(1 - 6\lambda f_\infty + 9\mu f_\infty^2\right)\,. \tag{3.9}$$

Given these results in eqs. (3.8) and (3.9), we also have

$$\frac{c-a}{c} = \frac{4 f_\infty(\lambda - 3\mu f_\infty)}{1 - 2\lambda f_\infty - 3\mu f_\infty^2}\,. \tag{3.10}$$

3.2 Two-point function

Now we turn to computing the two-point function of the stress tensor as an alternative approach to determining the central charge c. It is known [46–49, 52] that in a four-dimensional CFT[2]

$$\langle\, T_{ab}(x)\, T_{cd}(x') \,\rangle = \frac{C_T}{(x-x')^8}\, \mathcal{I}_{ab,cd}(x - x') \tag{3.11}$$

[2]We assume a Minkowski signature for the metric. Hence in eq. (3.12), $x_a = \eta_{ab} x^b$ (i.e., $x_0 = -t$).

JHEP08(2010)035

where

$$\mathcal{I}_{ab,cd}(x) = \frac{1}{2}\left(I_{ac}(x)I_{bd}(x) + I_{ad}(x)I_{bc}(x)\right) - \frac{1}{4}\eta_{ab}\eta_{cd}$$
$$\text{and} \quad I_{ab}(x) = \eta_{ab} - 2\frac{x_a x_b}{x^2}\,. \tag{3.12}$$

This structure is completely dictated by the constraints imposed by conformal symmetry [49, 52]. The coefficient C_T is related to the central charge c which appears as the coefficient of the (Weyl)^2 term in the trace anomaly (3.1):

$$C_T = \frac{40}{\pi^4}\,c\,. \tag{3.13}$$

In order to compute C_T, it is sufficient to focus on the specific case $\langle\, T_{xy}\, T_{xy}\,\rangle$. To determine this two-point function, we will turn on a perturbation $r^2 h_{xy}(r,z)/L^2$ in the AdS_5 background, i.e., in eq. (2.6) after setting $r_0 = 0$. The quadratic action for $h_{xy} = \phi$ can be written as

$$I_2 = \frac{1}{2\ell_{\rm P}^3}\int d^5x\left(K_r(\partial_r\phi)^2 + K_z(\partial_z\phi)^2 + \partial_r\Gamma\right)\,, \tag{3.14}$$

where

$$K_r = -\frac{r^5 f_\infty^{1/2}}{2L^5}\left(1 - 2\lambda f_\infty - 3\mu f_\infty^2\right), \tag{3.15}$$
$$K_z = -\frac{r}{2f_\infty^{1/2}L}\left(1 - 2\lambda f_\infty - 3\mu f_\infty^2\right). \tag{3.16}$$

The details of Γ are unimportant since the $\partial_r\Gamma$ contribution is canceled by a generalized Gibbons-Hawking boundary term [6]. Upon making the ansatz

$$\phi = e^{ipz}H_p(r)\,, \tag{3.17}$$

the equation of motion for ϕ reduces to

$$H_p''(r) + \frac{5}{r}H_p'(r) - \frac{L^4p^2}{f_\infty r^4}H_p(r) = 0\,. \tag{3.18}$$

The general solution can be written as

$$H_p(r) = C_1\,\frac{1}{r^2}\,K_2\!\left(\frac{L^2p}{f_\infty^{1/2}r}\right) + C_2\,\frac{1}{r^2}\,I_2\!\left(\frac{L^2p}{f_\infty^{1/2}r}\right)\,, \tag{3.19}$$

where $I_2(x)$ and $K_2(x)$ are modified Bessel functions of the first and second kind, respectively. In order to fix $H_p(r=\infty) = 1$, we set $C_1 = p^2L^4/(2f_\infty)$ and $C_2 = 0$. Using the equations of motion, eq. (3.14) can then be rewritten as

$$I_2 = \frac{1}{2\ell_{\rm P}^3}\int d^5x\,\partial_r(K_r\phi\,\partial_r\phi)\,. \tag{3.20}$$

JHEP08(2010)035

Substituting in the solution, we make a Fourier transform and extract the term proportional to $\log|p|$, which amounts to ignoring all contact terms:

$$\langle T_{xy}\, T_{xy}\rangle(p) = \frac{L^3}{8\ell_{\rm P}^3 f_\infty^{3/2}}(1-2\lambda f_\infty - 3\mu f_\infty^2)\, p^4 \log|p|\,. \tag{3.21}$$

In order to compare the above result with eq. (3.11), it convenient to recast the latter in Fourier space following [53]. We re-express the two-point function as [52]

$$\langle T_{ab}(x)\, T_{cd}(x')\rangle = \frac{C_T}{40}\,\mathcal{E}^{C\ ef}_{ab}{}_{,cd}{}^{gh}\,\partial_e\partial_f\,\partial'_g\partial'_h\,\frac{1}{(x-x')^4}\,, \tag{3.22}$$

where the tensor $\mathcal{E}^C$ satisfies

$$\begin{aligned}\mathcal{E}^{C}_{abef\,,cdgh}\,k^e k^f k^g k^h = \frac{1}{24}\Big(&2\,k_a k_b k_c k_d - \frac{3}{2}k^2(k_a k_c\eta_{bd}+k_b k_c\eta_{ad}+k_a k_d\eta_{bc}+k_b k_d\eta_{ac}) \\ &+k^2(k_a k_b\eta_{cd}+k_c k_d\eta_{ab})+\frac{3}{2}(k^2)^2(\eta_{ac}\eta_{bd}+\eta_{ad}\eta_{bc})-(k^2)^2\eta_{ab}\eta_{cd}\Big)\,.\end{aligned} \tag{3.23}$$

In the case of interest with $(ab) = (xy) = (cd)$, the factor involving $\mathcal{E}^C$ and the four derivatives simply evaluates to

$$p^4/16\,. \tag{3.24}$$

Hence in momentum space, the two-point function can be written as [53]

$$\langle T_{xy}\, T_{xy}\rangle(p) = \frac{C_T}{640}\,p^4\int d^4x\,\frac{e^{ip\cdot x}}{x^4} = \frac{\pi^2\, C_T}{320}\,p^4\,\log|p| + (\text{analytic in } p)\,. \tag{3.25}$$

Comparing eqs. (3.21) and (3.25), we find

$$C_T = \frac{40}{\pi^2}\,\frac{L^3}{\ell_{\rm P}^3}\,\frac{1}{f_\infty^{3/2}}(1-2\lambda f_\infty - 3\mu f_\infty^2) \tag{3.26}$$

and finally using eq. (3.13), we have

$$c = \pi^2\frac{L^3}{\ell_{\rm P}^3}\,\frac{1}{f_\infty^{3/2}}\left(1-2\lambda f_\infty - 3\mu f_\infty^2\right)\,. \tag{3.27}$$

This expression precisely matches that in eq. (3.8) which was found using the holographic trace anomaly in the previous section.

4 Holographic computation of energy fluxes

At this point, our holographic dictionary contains two entries. That is, eqs. (3.8) and (3.9) relating the central charges of the four-dimensional CFT to the couplings of the five-dimensional bulk gravity theory. However, the quasi-topological gravity (2.1) is characterized by three independent dimensionless parameters: λ, μ and $L/\ell_{\rm P}$. Hence we need to extend the dictionary further by identifying additional parameters which play an analogous universal role in the dual CFT. Further, since we are only dealing with the gravitational

JHEP08(2010)035

sector of the AdS_5 theory, we must find parameters governing the behaviour of the stress tensor in the CFT. A natural next step is to consider the three-point function of T_{ij}, as was extensively studied by [49, 52]. There it was shown that conformal symmetry and energy conservation are powerful enough to determine the the three-point function up to three constants, which are labeled $\mathcal{A}$, $\mathcal{B}$ and $\mathcal{C}$ in [52]. In fact, the two central charges can be expressed in terms of these three parameters, as we will elucidate below — see eqs. (4.35) and (4.36). Further as discussed in [13], constructing a holographic model which can explore the full range of these CFT parameters requires the introduction of curvature-squared and curvature-cubed interactions in the bulk gravity theory. In fact, this was the primary motivation for constructing the quasi-topological gravity theory.

One can perform a holographic calculation of the full three-point function [39], however, extending these calculations to quasi-topological gravity proves to be extremely challenging. Therefore, we choose an indirect route to determining these coefficients here. In particular, we construct a holographic description of a particular thought experiment proposed for four-dimensional CFT's in [13]. The experiment consists of first producing a disturbance, which is localized and injects a fixed energy, with an insertion of the stress tensor $\varepsilon_{ij}\, T^{ij}$, where ε_{ij} is a constant polarization tensor. Then one measures the energy flux escaping to null infinity in the direction indicated by the unit vector $\mathbf{n}$. The final result takes the form

$$\langle \mathcal{E}(\mathbf{n}) \rangle = \frac{E}{4\pi} \left[1 + t_2 \left(\frac{\varepsilon^*_{ij} \varepsilon_{ik} n^j n^k}{\varepsilon^*_{ij} \varepsilon_{ij}} - \frac{1}{3} \right) + t_4 \left(\frac{|\varepsilon_{ij} n^i n^j|^2}{\varepsilon^*_{ij} \varepsilon_{ij}} - \frac{2}{15} \right) \right] , \tag{4.1}$$

where E is the total energy. The structure of this expression is completely dictated by the symmetry of the construction. Hence the two constant coefficients, t_2 and t_4, are parameters that characterize the underlying CFT. Our holographic computation of t_2 and t_4 will extend our AdS/CFT dictionary to the point where the three independent gravitational couplings will be related to three independent parameters in the dual CFT.

Note that the (negative) constants appearing in eq. (4.1) in the two factors multiplied by t_2 and t_4 were chosen so that these factors contribute zero net flux when integrated over all directions. The negative sign of these constants leads to interesting constraints on the coefficients t_2 and t_4, which we discuss below in section 5.2.

4.1 Field theory calculations

Let us first consider the discussion of [13] in more detail. Again, we begin by making a small localized perturbation of the CFT in Minkowski space with metric $ds^2 = -dt^2 + \delta_{ij} dx^i dx^j$. With time this perturbation spreads out, and sufficiently far away one may imagine taking successively larger concentric two-spheres through which one is measuring the energy flux. Let us parameterize the points on these two spheres by a radius r (i.e., $r^2 = x_i x^i$ as usual) and a unit vector $\mathbf{n} = (n^1, n^2, n^3)$. Then the energy flux measured in the direction given by $\mathbf{n}$ is given by

$$\mathcal{E}(\mathbf{n}) = \lim_{r \to +\infty} r^2 \int_{-\infty}^{+\infty} dt\; T^t{}_i(t, r\,\mathbf{n})\; n^i \,. \tag{4.2}$$

As it stands, the flux in eq. (4.2) includes contributions from both the past and future null boundaries of Minkowski space. To separate out the future contribution which we

JHEP08(2010)035

are interested in, we select one of the coordinates x^3 and construct light-cone coordinates $x^\pm = t \pm x^3$. Then it is clear that the integral above has two contributions, namely one from future null infinity $x^+ \to +\infty$ and another one from past null infinity $x^- \to -\infty$. We will take only the former.[3] For large r, it is convenient to write

$$r^2 = (x^+ - x^-)^2 + (x^1)^2 + (x^2)^2 \quad \stackrel{x^+ \to +\infty}{\longrightarrow} \quad (x^+)^2 (1 + (y^1)^2 + (y^2)^2), \quad \text{where} \quad y^{1,2} \equiv x^{1,2}/x^+ .$$

Therefore we obtain

$$\mathcal{E}(\mathbf{n}) = - \lim_{x^+ \to +\infty} (x^+)^2 \left(1 + (y^1)^2 + (y^2)^2\right) \int_{-\infty}^{+\infty} dx^- \left[T_{+i}(x^+, x^-, \mathbf{n}) + T_{-i}(x^+, x^-, \mathbf{n}) \right] n^i . \tag{4.3}$$

Motivated by the preceding, we define new coordinates y^a:

$$y^+ = -\frac{1}{x^+} , \quad y^- = x^- - \frac{(x^1)^2 + (x^2)^2}{x^+} , \quad y^{1,2} = \frac{x^{1,2}}{x^+} . \tag{4.4}$$

In terms of these coordinates, the desired energy flux is measured $y^+ = 0$. Further it is not difficult to show that on this surface, we have

$$y^{1,2} = \frac{n^{1,2}}{1 + n^3} . \tag{4.5}$$

Now we transform the energy momentum tensor from x^a to y^a coordinates, as usual

$$T^x_{ab} = \frac{\partial y^c}{\partial x^a} \frac{\partial y^d}{\partial x^b} T^y_{cd} . \tag{4.6}$$

Here we are simplifying our notation with the superscripts, x and y, to indicate in which coordinate system the stress tensor is written, i.e., $T^y_{--} = T_{y^- y^-}$. Now at $y^+ = 0$, we obtain

$$\begin{aligned} T^x_{++} &= \left((y^1)^2 + (y^2)^2\right)^2 T^y_{--} , \quad T^x_{+\,1,2} = -2\, y^{1,2} \left((y^1)^2 + (y^2)^2\right) T^y_{--} , \\ T^x_{+-} &= \left((y^1)^2 + (y^2)^2\right) T^y_{--} , \quad T^x_{--} = T^y_{--} , \quad T^x_{-\,1,2} = -2\, y^{1,2}\, T^y_{--} . \end{aligned} \tag{4.7}$$

Hence we see that on this surface (i.e., $y^+ = 0$), there is a single relevant component of the energy momentum tensor in y coordinates. Using these relations, we rewrite eq. (4.3) as:

$$\mathcal{E}(\mathbf{n}) = \Omega^3 \int_{-\infty}^{+\infty} dy^- \, \frac{T^y_{--}(y^+ = 0, y^-, y^1, y^2)}{(y^+)^2} \tag{4.8}$$

with $\Omega = 2/(1 + n^3)$.

Further, we note that transforming from the x^a to y^a coordinates produces a Weyl scaling of the metric. Hence it is natural to use this transformation to perform the conformal transformation:

$$\begin{aligned} \mathrm{d}s^2 &= -\mathrm{d}x^+ \mathrm{d}x^- + (\mathrm{d}x^1)^2 + (\mathrm{d}x^2)^2 = \frac{-\mathrm{d}y^+ \mathrm{d}y^- + (\mathrm{d}y^1)^2 + (\mathrm{d}y^2)^2}{(y^+)^2} \\ \longrightarrow \qquad \mathrm{d}\tilde{s}^2 &= -\mathrm{d}y^+ \mathrm{d}y^- + (\mathrm{d}y^1)^2 + (\mathrm{d}y^2)^2 . \end{aligned} \tag{4.9}$$

[3] Note that the following discussion overlooks the flux contribution on the 'hemisphere' at $x^- \to +\infty$. However, our primary concern is the functional dependence of $\mathcal{E}(\mathbf{n})$ and so this does not affect our results.

JHEP08(2010)035

Then the energy momentum tensor transforms

$$\tilde{T}_{ab} = \left|\frac{\partial x}{\partial y}\right|^{-1/2} \frac{\partial x^c}{\partial y^a}\frac{\partial x^d}{\partial y^b} T_{cd}\,. \tag{4.10}$$

In particular, we have $\tilde{T}^y_{--} = T^y_{--}/(y^+)^2$ and therefore eq. (4.8) becomes:

$$\mathcal{E}(\mathbf{n}) = \Omega^3 \int_{-\infty}^{+\infty} dy^-\ \tilde{T}^y_{--}(y^+ = 0, y^-, y^1, y^2). \tag{4.11}$$

Following [13], we wish to consider the expectation value of this flux operator $\mathcal{E}(\mathbf{n})$ for a particular state

$$\langle \mathcal{E}(\mathbf{n})\rangle = \frac{\langle 0|\,\mathcal{O}_{\rm E}^\dagger\,\mathcal{E}(\mathbf{n})\,\mathcal{O}_{\rm E}\,|0\rangle}{\langle 0|\,\mathcal{O}_{\rm E}^\dagger\,\mathcal{O}_{\rm E}\,|0\rangle}\,. \tag{4.12}$$

In the present discussion, the operator $\mathcal{O}_{\rm E}$ is assumed to be a localized insertion of the stress tensor of the form

$$\mathcal{O}_{\rm E} = \int d^4x\,\varepsilon^{ij}\,T_{ij}\,e^{-iEt}\,\psi(x/\sigma)\,. \tag{4.13}$$

Here $\psi(x/\sigma)$ is some profile which localizes the insertion to $x^a = 0$ on the scale σ. We assume $E \gg 1/\sigma$ and so the energy of the insertion is E up to order $1/\sigma$ corrections. Finally since the stress tensor enters this construction, the operator also contains a constant polarization tensor ε_{ij} which we assume only has spatial components. The symmetry of this construction then dictates that the flux expectation value (4.12) takes the form given in eq. (4.1). Further, it is clear that by construction the result is completely determined by the three-point function of the stress tensor. Hence the flux parameters t_2 and t_4 appearing in eq. (4.1) will be related to $\mathcal{A}$, $\mathcal{B}$ and $\mathcal{C}$, the parameters controlling this three-point function.

4.2 Holographic calculations

The x^a and y^a coordinates defined in the previous section are easily extended into the AdS_5 bulk with

$$\mathrm{d}s^2 = \frac{\tilde{L}^2}{z^2}\left(-\mathrm{d}x^+\mathrm{d}x^- + (\mathrm{d}x^1)^2 + (\mathrm{d}x^2)^2 + \mathrm{d}z^2\right) \tag{4.14}$$

$$= \frac{\tilde{L}^2}{u^2}\left(-\mathrm{d}y^+\mathrm{d}y^- + (\mathrm{d}y^1)^2 + (\mathrm{d}y^2)^2 + \mathrm{d}u^2\right)\,. \tag{4.15}$$

Recall that $\tilde{L}$ is the curvature of the AdS_5 geometry, as defined in eq. (2.4). To relate these two coordinate systems, it is convenient to describe AdS_5 as the hyperbola

$$-(W^{-1})^2 - (W^0)^2 + (W^1)^2 + (W^3)^2 + (W^3)^2 + (W^4)^2 = -\tilde{L}^2 \tag{4.16}$$

in a six-dimensional Minkowski space with (–,–,+,+,+,+) signature. Note that we reach the boundary of AdS_5 by taking W^M large. The previous coordinates are mapped to the W^M coordinates with

$$W^{-1} + W^4 = \frac{\tilde{L}^2}{z}\,, \qquad W^a = \tilde{L}\,\frac{x^a}{z} \quad \text{for } a = 0,1,2,3\,, \tag{4.17}$$

$$W^0 + W^3 = \frac{\tilde{L}}{u}\,, \quad W^{-1} + W^4 = -\tilde{L}^2\,\frac{y^+}{u}\,, \quad W^{-1} - W^4 = -\frac{y^-}{u}\,, \quad W^{1,2} = \tilde{L}\,\frac{y^{1,2}}{u}\,.$$

JHEP08(2010)035

Note that z and u are mapped to two orthogonal null surfaces in the W^M space. Further the powers of $\tilde{L}$ are slightly different in the second line above to ensure that the (engineering) dimension of the coordinates is properly accounted for, i.e., u is dimensionless while y^+ has dimensions $length^{-1}$. With eq.(4.17), we can relate the (x^a, z) and (y^a, u) coordinate systems in eqs. (4.14) and (4.15) as

$$\begin{aligned} y^+ &= -\frac{1}{x^+}\,, \qquad y^{1,2} = \frac{x^{1,2}}{x^+}\,, \qquad u = \frac{z}{x^+}\,, \\ y^- &= x^- - \frac{(x^1)^2 + (x^2)^2}{x^+} - \frac{z^2}{x^+}\,. \end{aligned} \tag{4.18}$$

Notice that on the asymptotic boundary $z = 0$, the above coordinate transformation reduces to that given in eq. (4.4). Further with $y^+ = 0$ and any finite value of u, we are on the AdS_5 horizon at $z = \infty$ in the (x^a, z) coordinates.

As commented above, in calculating the flux expectation value in eq. (4.12), we are essentially determining a specific component of the three-point function of the stress tensor. Hence in our holographic description, we must first introduce appropriate metric perturbations $h_{\mu\nu}$ in the AdS_5 bulk which couple to the dual insertions of T_{ab}. We then evaluate the on-shell contribution to the cubic effective action for the graviton insertions.

As discussed in [36], in general, the equations of motion for quasi-topological gravity involve higher derivatives. Hence one would expect that linearized equations of motion for the metric perturbations here are also higher order. However, it was observed in [36] that in fact these linearized equations for gravitons propagating in the AdS_5 vacuum match precisely the second order equations of Einstein's theory, up to some overall (constant) coefficient, as shown in eq. (2.10). This makes the following calculations much simpler as we may borrow previous results [13, 39] for the graviton solutions in Einstein gravity. Hence while the higher derivative contributions in quasi-topological gravity are essential to producing a nonvanishing value for t_4 in the dual CFT, they only contribute through the three-point interactions in the following.

We first consider the flux operator $\mathcal{E}(\mathbf{n})$ in eq. (4.11). It is natural to use the (y^a, u) coordinates in eq. (4.15) and the standard AdS/CFT dictionary advises us that $\tilde{T}^y{}_{--}(y)$ couples to $h_{++}(y^a, u = 0)$. Considering first a localized insertion $h_{++}(y^a, u = 0) = \delta(y^1)\delta(y^2)\delta(y^+)$, the bulk solution is given by

$$h_{++}(y^+, y^-, y^1, y^2, u) = \frac{u^2}{(u^2 - y^+(y^- - y'^-) + (y^1)^2 + (y^2)^2)^4}\,. \tag{4.19}$$

As noted above, we are using the same solution here as in [13] because the linearized equations of motion for perturbations around AdS_5 in quasi-topological gravity are the same for Einstein gravity [36]. To obtain the operator $\mathcal{E}(\mathbf{n})$, we then integrate in y^-, as well as multiplying by an overall factor of Ω^3 and performing a translation in y^1 and y^2, to obtain

$$h_{++}(y^+, y^1, y^2, u) = \frac{8\,\delta(y^+)}{(1+n_3)^3}\,\frac{u^2}{(u^2 + (y^1 - y'^1)^2 + (y^2 - y'^2)^2)^3}\,, \tag{4.20}$$

with $y'^{1,2} = n^{1,2}/(1+n^3)$, as in eq. (4.5).

JHEP08(2010)035

In fact we can make this insertion at a nonlinear level in the bulk gravity theory, following [13] and [14]. To achieve this, we consider the shockwave background:

$$ds^2 = \frac{\tilde{L}^2}{u^2}\Big[\,\delta(y^+)\,\mathcal{W}(y^1,y^2,u)(dy^+)^2 - dy^+dy^- + (dy^1)^2 + (dy^2)^2 + du^2\Big] \tag{4.21}$$

This metric solves the full equations of motion coming from eq. (2.1) provided that $\mathcal{W}(y^1,y^2,u)$ satisfies the equation of motion

$$\partial_u^2\mathcal{W} - \frac{3}{u}\,\partial_u\mathcal{W} + \partial_{y^1}^2\mathcal{W} + \partial_{y^2}^2\mathcal{W} = 0\,. \tag{4.22}$$

This simple linear equation appears as the equation of motion in Einstein gravity and one can readily show that it is not corrected by the higher curvature terms in eq. (2.1) with the arguments of [54, 55]. From our expression for h_{++} in eq. (4.20), the relevant wavefunction is

$$\mathcal{W}(y^1,y^2,u) = \frac{\Omega^3}{\tilde{L}^2}\,\frac{u^4}{\left(u^2+(y^1-y'^1)^2+(y^2-y'^2)^2\right)^3} \tag{4.23}$$

with $y'^{1,2} = n^{1,2}/(1+n^3)$, as before.

Next we turn to the graviton perturbations dual to the operator insertion $\mathcal{O}_{\rm E}$ in eq. (4.13). To simplify the discussion, we choose a particular polarization with $\varepsilon_{x^1x^2} = 1 = \varepsilon_{x^2x^1}$ and all other components vanishing. Using the (x^a,z) coordinate system in eq. (4.14), the desired operator (4.13) is sourced by a metric perturbation with the boundary value: $h_{x^1x^2}(x^a, z\to 0) = z^{-2}e^{-iE(x^+ + x^-)/2}$. The bulk solution that corresponds to this boundary perturbation is then

$$h_{x^1x^2}(x^a,z) = \int d^4x'\, e^{-i\frac{E}{2}(x'^+ + x'^-)}\,\frac{1}{(z^2+(x-x')^2)^2}\,. \tag{4.24}$$

Since the h_{++} perturbation is completely localised at $y^+ = 0$, for later purposes, we will primarily be interested in the behaviour of $h_{x^1x^2}(x^a,z)$ on that surface. Following [13], it is possible to perform the above integral using the parameterization of AdS_5 in eq. (4.16) to produce

$$h_{x^1x^2}(W^+\simeq 0, W^-, W^i) \simeq \frac{(W^+)^2}{\tilde{L}^4E^2}\,e^{-iEW^-/2}\delta^3(W^i)\,, \tag{4.25}$$

where $W^\pm = W^{-1}\pm W^4$. Implicitly, W^0 has been replaced with $(W^0)^2 = 1-(W^i)^2$ which is the reduction of eq. (4.16) with $W^+ = 0$. Using eq. (4.17), we may express the coordinate dependence in terms of (y^a,u)

$$h_{x^1x^2}(y^+\simeq 0, y^-, y^1, y^2, u) \simeq \frac{(y^+)^2}{E^2}\,e^{iEy^-/2}\;\delta(y^1)\;\delta(y^2)\;\delta(u-1)\,. \tag{4.26}$$

Finally with the coordinate transformation (4.18), we also transform the tensor indices to find that at $y^+\to 0$, our metric perturbation becomes

$$h_{y^1y^2} \simeq \frac{1}{E^2}\,e^{iEy^-/2}\;\delta(y^1)\;\delta(y^2)\;\delta(u-1) \tag{4.27}$$

along with other $h_{y^+y^1}$, $h_{y^+y^2}$ and $h_{y^+y^+}$ components. However, the form of the latter will not be important, as we now discuss. Note that the original expression (4.24) was

JHEP08(2010)035

transverse and traceless in the (x^a, z) coordinates but as a result, the expression produced by simply making a coordinate transformation to the (y^a, u) coordinates is not. However, it is convenient to work in this gauge since a great simplification results in the equation of motion for the graviton propagating in the AdS_5 background, i.e., away from the shockwave deformation in eq. (4.21). Hence at this point, we choose add to eq. (4.27) the components required to impose transverse traceless gauge in the (y^a, u) coordinates.

The mode above was traceless by construction and so we only need to ensure that the transverse condition is satisfied as well, i.e., $\nabla^\mu h_{\mu\nu} = 0$. In the present case, the latter can be satisfied as long as $h_{y^1y^2}$ is accompanied by modes satisfying:

$$\begin{aligned} \partial_{y^-} h_{y^+y^1} &= \frac{1}{2}\,\partial_{y^2} h_{y^2y^1}\,, \quad \partial_{y^-} h_{y^+y^2} = \frac{1}{2}\,\partial_{y^1} h_{y^1y^2}\,, \\ \partial_{y^-} h_{y^+y^+} &= \frac{1}{2}\left(\partial_{y^1} h_{y^1y^+} + \partial_{y^2} h_{y^2y^+}\right)\,. \end{aligned} \tag{4.28}$$

Together the $h_{y^1y^2}$, $h_{y^+y^1}$, $h_{y^+y^2}$ and $h_{y^+y^+}$ components form an independent transverse traceless mode. We have verified that with $h_{y^1y^2}(y,u) \equiv \tilde{L}^2/u^2\,\phi(y,u)$ and the remaining components chosen to satisfy eq. (4.28), the equation of motion for $\phi(y,u)$ becomes simply that of a massless scalar in AdS_5 (up to interaction terms with the shockwave):

$$\partial_u^2\phi - \frac{3}{u}\,\partial_u\phi + \partial_{y^1}^2\phi + \partial_{y^2}^2\phi - 4\partial_{y^+}\partial_{y^-}\phi = 0\,. \tag{4.29}$$

To find the three-point function, we add these perturbations to the metric (4.21) and evaluate the action (2.1) on-shell. Then we must extract the terms of the form $\mathcal{W}\,\phi^2$ from this result. After integration by parts and using the equations of motion, the cubic effective action becomes

$$S^{(3)}_{\mathcal{W}\phi^2} = -\frac{1}{8\ell_{\rm P}^3}\int d^5x\sqrt{-g}\;\phi\;\partial_-^2\phi\;\mathcal{W}\Big[1 - 2f_\infty\lambda - 3\mu f_\infty^2 + f_\infty(\lambda - 87 f_\infty\mu)\,T_2 + 21 f_\infty^2\mu\,T_4\Big] \tag{4.30}$$

where

$$\begin{aligned} T_2 &= \left.\frac{\partial_1^2\mathcal{W} + \partial_2^2\mathcal{W} - 2\,\partial_u\mathcal{W}}{\mathcal{W}}\right|_{u=1,\,y^1=y^2=0}\,, \\ T_4 &= \left.\left(3\,T_2 + \frac{\partial_1^2\partial_2^2\mathcal{W} - \partial_u\partial_1^2\mathcal{W} - \partial_u\partial_2^2\mathcal{W}}{\mathcal{W}}\right)\right|_{u=1,\,y^1=y^2=0}\,. \end{aligned} \tag{4.31}$$

Implicitly here, we are using that with the perturbations given above, i.e., eqs. (4.20) and (4.26), the interaction is entirely localized along $y^+ = 0 = y^1 = y^2$ and $u = 1$. Substituting the solution (4.23) for $\mathcal{W}(y^1, y^2, u)$ into eq. (4.31), we obtain

$$T_2 = 24\left(\frac{n_1^2 + n_2^2}{2} - \frac{1}{3}\right) \qquad T_4 = 180\left(2\,n_1^2\,n_2^2 - \frac{2}{15}\right)\,. \tag{4.32}$$

The expressions above involving n^1 and n^2 should be interpreted as two independent SO(3)-invariant combinations of the unit vector n^i and the (implicit) polarization tensor ε_{ij}, i.e.,

$$\frac{n_1^2 + n_2^2}{2} = \frac{\varepsilon^*_{ij}\,\varepsilon_{ik}\,n^j n^k}{\varepsilon^*_{ij}\,\varepsilon_{ij}}\,, \qquad 2n_1^2 n_2^2 = \frac{|\varepsilon_{ij}\,n^i n^j|^2}{\varepsilon^*_{ij}\,\varepsilon_{ij}}\,. \tag{4.33}$$

JHEP08(2010)035

This was the guiding principle in selecting the two combinations presented in eq. (4.31). To normalize the final result, we must divide by the two-point function $\langle T_{y^1y^2}\, T_{y^1y^2}\rangle$, which is essentially the calculation of section 3.2. We finally arrive at an expression identical to that in eq. (4.1) with

$$t_2 = \frac{24 f_\infty(\lambda - 87 f_\infty \mu)}{1 - 2 f_\infty \lambda - 3 f_\infty^2 \mu}\,, \qquad t_4 = \frac{3780 f_\infty^2 \mu}{1 - 2 f_\infty \lambda - 3 f_\infty^2 \mu}\,. \tag{4.34}$$

4.3 General three-point parameters

At this point, we return to $\mathcal{A}$, $\mathcal{B}$ and $\mathcal{C}$, the parameters in the dual CFT controlling the general structure of the three-point function of the stress tensor [49, 52]. In fact, these parameters fix both the central charges, c and a, and the flux parameters, t_2 and t_4, in the CFT. Hence we can use the results in the previous section and in section 3 to express the three-point parameters in terms of the gravitational couplings.

First, we can express the central charges as [49]

$$c = \frac{\pi^6}{480}\,(9\mathcal{A} - \mathcal{B} - 10\mathcal{C})\,, \tag{4.35}$$

$$a = \frac{\pi^6}{2880}\,(13\mathcal{A} - 2\mathcal{B} - 40\mathcal{C})\,. \tag{4.36}$$

Further we have [13, 20]

$$t_2 = \frac{15(5\mathcal{A} + 4\mathcal{B} - 12\mathcal{C})}{9\mathcal{A} - \mathcal{B} - 10\mathcal{C}}\,, \qquad t_4 = -\frac{15(17\mathcal{A} + 32\mathcal{B} - 80\mathcal{C})}{4(9\mathcal{A} - \mathcal{B} - 10\mathcal{C})}\,. \tag{4.37}$$

Given that these four quantities are all determined by the same three parameters, these expressions must be redundant. That is, we can see that there is a consistency condition:

$$\frac{c-a}{c} = \frac{1}{6}t_2 + \frac{4}{45}t_4 = \frac{41\mathcal{A} - 4\mathcal{B} - 20\mathcal{C}}{6(9\mathcal{A} - \mathcal{B} - 10\mathcal{C})}\,. \tag{4.38}$$

With the results (4.34) in the previous section,

$$\frac{1}{6}t_2 + \frac{4}{45}t_4 = \frac{4 f_\infty(\lambda - 3\mu f_\infty)}{1 - 2\lambda f_\infty - 3\mu f_\infty^2}\,. \tag{4.39}$$

Now comparing to eq. (3.10), we see that our holographic results satisfy the required relation (4.38).

Combining these expressions (4.35)–(4.37) with the results of the holographic calculations, eqs. (4.34), (4.35) and (4.36), we arrive at the following expressions

$$\mathcal{A} = -\frac{512}{9\pi^4}\frac{L^3}{\ell_{\rm P}^3}\frac{1}{f_\infty^{3/2}}\left(1 - 12\lambda f_\infty + 48\mu f_\infty^2\right)\,, \tag{4.40}$$

$$\mathcal{B} = -\frac{32}{9\pi^4}\frac{L^3}{\ell_{\rm P}^3}\frac{1}{f_\infty^{3/2}}\left(49 - 318\lambda f_\infty + 4377\mu f_\infty^2\right)\,, \tag{4.41}$$

$$\mathcal{C} = -\frac{32}{9\pi^4}\frac{L^3}{\ell_{\rm P}^3}\frac{1}{f_\infty^{3/2}}\left(23 - 168\lambda f_\infty + 213\mu f_\infty^2\right)\,. \tag{4.42}$$

JHEP08(2010)035

5 Physical constraints

Having established several interesting entries in the AdS/CFT dictionary for quasi-topological gravity, we next consider various constraints on the gravitational couplings that arise to ensure the physical consistency of the dual CFT's. We consider three independent constraints in the following:

5.1 Positivity of C_T

Unitarity of the CFT requires that the central charge C_T or c is positive. This constraint on c may seem somewhat mysterious from the point of view of the holographic trace anomaly discussed in section 3.1. However, the definition in section 3.2 shows C_T appears in the two-point function and so this central charge controls the sign of the norm of CFT states created with the stress tensor. Hence given eq. (3.26), the dual gravity theory must satisfy

$$1 - 2f_\infty\,\lambda - 3f_\infty^2\,\mu > 0\,. \tag{5.1}$$

At this point, we note that multiplying the expression on the left-hand side of eq. (5.1) by minus one yields precisely the derivative of the left-hand side of eq. (2.5), i.e., the slope of the polynomial there evaluated at the root given by eq. (2.5). This comment is related to the observation in [36] that this slope appears as a pre-factor in the kinetic term for graviton or in the linearized equations of motion (2.10) in the AdS vacua of the theory. That is, the sign of the slope determines whether or not the graviton is a ghost in a particular AdS vacuum — the graviton is well-behaved when the slope is negative. Of course, the holographic calculation in section 3.2 shows that C_T is precisely determined by the graviton propagator and so it is no surprise that the same factor appears in both places. Further, we note that in AdS vacua with a ghost-like graviton, this pathology would make a prominent appearance as non-unitarity in the dual CFT since C_T would be negative. The analogous observations were made for GB gravity in [20].

5.2 Positivity of energy fluxes

Turning to the expression of the energy flux in eq. (4.1), we note that the two factors multiplied by t_2 and t_4 were normalized to give a vanishing contribution to the net flux when integrated over all directions. Hence depending on the specific direction, these factors may give either a positive or negative contribution to $\langle \mathcal{E}(\mathbf{n})\rangle$. Further, it is easy to see that if the coefficients t_2 and t_4 become too large, the energy flux measured in various directions will become negative. Following [13], avoiding this problem then imposes various constraints on these coefficients:[4]

$$\text{Tensor}: \quad 1 - \frac{1}{3}t_2 - \frac{2}{15}t_4 \geq 0\,, \tag{5.2}$$

$$\text{Vector}: \quad 1 + \frac{1}{6}t_2 - \frac{2}{15}t_4 \geq 0\,, \tag{5.3}$$

$$\text{Scalar}: \quad 1 + \frac{1}{3}t_2 + \frac{8}{15}t_4 \geq 0\,. \tag{5.4}$$

[4] A complementary analysis in [56] produced a constraint equivalent to eq. (5.4), again as a positivity constraint on the three-point function of the stress tensor.

JHEP08(2010)035

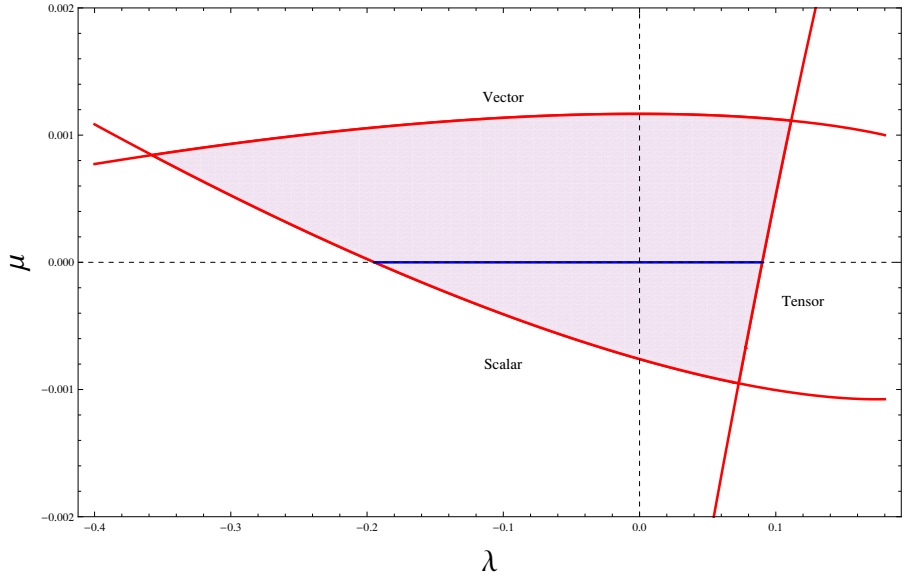

Figure 1. The allowed region in (λ, μ)-plane satisfying the constraints appearing in eqs. (5.5)–(5.7). Within this region, the energy flux (4.1) in the dual CFT is positive for any direction. The (blue) segment on the λ-axis within the allowed region matches precisely the allowed values of the coupling in five-dimensional GB gravity.

If the polarization tensor is chosen with $\varepsilon_{x^1x^2} = 1 = \varepsilon_{x^2x^1}$ and all other components vanishing, as in section 4.2, the tensor, vector and scalar constraints above correspond to demanding a positive flux with $n_3^2 = 1$, $n_1^2 = 1$ (or $n_2^2 = 1$), and $n_1^2 = 1/2 = n_2^2$, respectively. Using eq. (4.34), we translate these constraints on t_2 and t_4 to constraints on the gravitational couplings:

$$\text{Tensor}: \quad 1 - 10 f_\infty \lambda + 189 f_\infty^2 \mu \geq 0\,, \tag{5.5}$$

$$\text{Vector}: \quad 1 + 2 f_\infty \lambda - 855 f_\infty^2 \mu \geq 0\,, \tag{5.6}$$

$$\text{Scalar}: \quad 1 + 6 f_\infty \lambda + 1317 f_\infty^2 \mu \geq 0\,. \tag{5.7}$$

In the present case, these constraints confine the higher curvature couplings of quasi-topological gravity to lie within a small region in the (λ, μ)-plane, as shown in figure 1.

Setting $\mu = 0$ reduces the theory to GB gravity and one recovers the expected constraints from eqs. (5.5)–(5.7) in this limit [14, 17]. First with $\mu = 0$, eq. (2.5) yields $f_\infty = \frac{1}{2\lambda}\left(1 - \sqrt{1 - 4\lambda}\right)$ for the ghost-free AdS vacuum. Then, for example, the tensor constraint (5.5) reduces to $5\sqrt{1 - 4\lambda} - 4 \geq 0$ or $\lambda \leq 9/100$. Similarly, the vector (5.6) and scalar (5.7) constraints yield $\lambda \geq -3/4$ and $\lambda \geq -7/36$, respectively. Hence to maintain positive energy fluxes in all directions, the curvature-squared coupling must lie in the range $-\frac{7}{36} \leq \lambda \leq \frac{9}{100}$, as expected [14, 17]. While the latter combines the results for the tensor and scalar constraints, the inequality arising from the vector constraint also matches the previously derived result [14, 17]. The allowed GB theories are illustrated in figure 1 as the blue segment on the λ-axis (i.e., $\mu = 0$) within the allowed region.

JHEP08(2010)035

5.3 Causality constraints

Constraining the gravitational couplings by demanding that the dual CFT respects causality was first explored in the context of five-dimensional Gauss-Bonnet gravity [15, 16]. In this analysis, one considers graviton fluctuations that probe the bulk geometry. The AdS_5 vacuum (i.e., eq. (2.6) with $f(r) = f_\infty$) is Lorentz invariant in the CFT directions and so no violations of causality would be found with this bulk spacetime. Instead, the black hole solution provides a background where Lorentz invariance is broken and in certain instances, the dual CFT plasma supports superluminal signals. Hence one constrains the gravitational couplings to avoid the appearance of such superluminal modes. The original analysis [15, 16] of GB gravity only considered gravitons polarized transversely to the momentum direction, in what is conventionally called the tensor channel. The analysis was later extended to the shear and sound channels in [14, 17]. These causality constraints have since been extended to GB gravity in higher dimensions [18–23] and more generally to higher order Lovelock theories [27–30].

In all of these cases, it was found that the causality constraints precisely match those arising from requiring positive energy fluxes. In particular, for five-dimensional GB theory, these constraints are exactly equivalent to those presented in eqs. (5.5)–(5.7) with $\mu = 0$. However, it has been shown that this matching does not appear in general, in particular for cases where the gravitational equations of motion are not second order [14]. Hence, in general, one has two independent sets of constraints, one required by the positive fluxes and a second determined by the absence of superluminal modes. In quasi-topological gravity, the linearized equations in a general background (and as we will see, in a black hole background) are fourth order in derivatives and so we do not expect that the previous constraints (5.5)–(5.7) will be reproduced by the causality analysis. However, unfortunately our final results here will be similar to those in [14]. That is, we find no evidence of causality violation once the curvature-cubed coupling μ is turned on in quasi-topological gravity.

There is a broad literature discussing causality in general field theories [57–59]. The key property characterizing how quickly signals propagate is the speed with which a wavefront propagates out from a discontinuity in some initial data. This front velocity is given by

$$v^{front} \equiv \lim_{|q|\to\infty} \mathrm{Re}(\omega)/q\,. \tag{5.8}$$

That is, we are interested in the phase velocity of modes in the limit of infinitesimally short wavelengths. Hence in a relativistic field theory, we would require that $v^{front} \leq 1$ in order to avoid any acausal behaviour.

In the present holographic framework, we need to determine the front velocity of signals in the dual CFT. That is, we must determine this velocity for excitations dual to various graviton channels in the bulk spacetime. Consider the black hole background given in eq. (2.6) and define the new coordinate $\rho = r_0^2/r^2$. The metric becomes

$$\mathrm{d}s^2 = \frac{r_0^2}{L^2\rho}\left(-\frac{f(\rho)}{f_\infty}\,\mathrm{d}t^2 + \mathrm{d}x_1^2 + \mathrm{d}x_2^2 + \mathrm{d}x_3^2\right) + \frac{L^2}{4\rho^2 f(\rho)}\,\mathrm{d}\rho^2\,. \tag{5.9}$$

JHEP08(2010)035

For simplicity, we will focus on tensor perturbations of the form

$$h_{x^1x^2} = \frac{r_0^2}{L^2\rho} e^{-i\omega t + iqx_3}\phi(\rho) \tag{5.10}$$

propagating on the background given in eq. (5.9). The determination of the front velocity for such modes was described in detail in [15]. For our present purposes, it suffices to derive the effective speed in the CFT directions at large momentum and frequency by focusing on the contributions coming from the t and z derivatives in the linearized equations of motion. That is, the full linearized equation for $\phi(\rho)$ takes the form

$$\partial_\rho\left(\mathcal{C}^{(2)}(\rho,q^2)\,\partial_\rho\phi(\rho)\right) + \mathcal{C}^{(0)}(\rho,q^2,\omega^2)\,\phi(\rho) = 0\,, \tag{5.11}$$

The function $\mathcal{C}^{(2)}$ contains two terms, one independent of q and the other proportional to q^2. In contrast, the $\mathcal{C}^{(0)}$ function is a sum of terms proportional to $\omega^2, q^2, \omega^2q^2$ and q^4. In the large momentum and frequency limit, the radial derivatives can be neglected and essentially only the $\mathcal{C}^{(0)}$ term is relevant above. By setting this term to zero, one finds an effective 'dispersion relation' relating the frequency to the momentum. As the final result is quite a complicated expression, let us approach it in several steps.

We start by setting both λ and μ to zero, in which case our theory reduces to Einstein gravity. Then the dispersion relation is simply

$$0 = \omega^2 - \frac{f(\rho)}{f_\infty}\,q^2\,. \tag{5.12}$$

For Einstein gravity, $f(\rho) = 1-\rho^2$ (and $f_\infty = 1$). Therefore the pre-factor multiplying q^2 above is less than one for any finite radius and we expect that these excitations always propagate at less than the speed of light, i.e., $\omega^2/q^2 \leq 1$. Next we consider GB gravity with $\lambda \neq 0$ and $\mu = 0$. In this case the dispersion relation becomes

$$0 = \omega^2\left(1-2\lambda f(\rho)+2\rho\lambda f'(\rho)\right) - \frac{f(\rho)}{f_\infty}\,q^2\left(1-2\lambda f(\rho)+2\lambda\rho f'(\rho)-4\rho^2\lambda f''(\rho)\right) \tag{5.13}$$

Using the GB black hole solutions and expanding the above expression near the AdS boundary yields

$$\frac{\omega^2}{q^2} = 1 - \frac{1-10f_\infty\lambda}{f_\infty(1-2f_\infty\lambda)^2}\,\rho^2 + \mathcal{O}\big(\rho^4\big)\,. \tag{5.14}$$

Hence we expect that preventing a superluminal front velocity requires $1-10f_\infty\lambda \geq 0$, which matches precisely the tensor constraint (5.5) with $\mu = 0$. Of course, this agreement for GB gravity was previously noted [13, 14, 17].

Now for the full theory with both $\lambda \neq 0$ and $\mu \neq 0$, the story is quite different. As described in [36], the linearized equations of motion describing gravitons in a general background for quasi-topological gravity are fourth order in derivatives. As a result, one finds that the equations for the tensor perturbations in the black hole background now involve higher powers of momentum, i.e., terms proportional to ω^2q^2 and q^4, as well as

JHEP08(2010)035

$q^2\partial_u^2$. These quartic momentum terms will then dominate the large q limit. Indeed, in this case the full effective dispersion relation becomes

$$\begin{aligned}
0 = {} & \omega^2\left(1-2\lambda f(\rho)+2\rho\lambda f'(\rho)\right)-\frac{f(\rho)}{f_\infty}\,q^2\left(1-2\lambda f(\rho)+2\lambda\rho f'(\rho)-4\rho^2\lambda f''(\rho)\right)\\
& -3\mu\,\omega^2\,\Big[f(\rho)\Big(f(\rho)-2\rho f'(\rho)+27\rho^2 f''(\rho)+48\rho^3 f^{(3)}(\rho)+12\rho^4 f^{(4)}(\rho)\Big)\\
& \qquad +3\rho^2 f'(\rho)\Big(f'(\rho)+6\rho\, f''(\rho)+2\rho^2 f^{(3)}(\rho)\Big)+6\rho^4 f''(\rho)^2\Big]\\
& +3\mu\,\frac{f(\rho)}{f_\infty}\,q^2\,\Big[f(\rho)\Big(f(\rho)-2\rho f'(\rho)-23\rho^2 f''(\rho)-48\rho^3 f^{(3)}(\rho)-12\rho^4 f^{(4)}(\rho)\Big)\\
& \qquad +\rho^2 f'(\rho)\Big(f'(\rho)-24\,\rho\, f''(\rho)-12\rho^2 f^{(3)}(\rho)\Big)\Big]\\
& -12\mu\,\rho^2\frac{f(\rho)}{f_\infty}\,q^2\Big(f'(\rho)+2\rho f''(\rho)\Big)\Big(\omega^2-\frac{f(\rho)}{f_\infty}q^2\Big)
\end{aligned}\tag{5.15}$$

Hence as commented above, in the limit of large q, the contributions from the higher momentum terms, appearing in the last line above, come to dominate. In fact then, the dispersion relation reduces to that found for Einstein gravity (5.12). Therefore we conclude that the dual excitations always propagate at less than the speed of light. A similar result was also found in [14] when considering a Weyl-tensor squared interaction added to the usual Einstein action.

However, one might find this analysis somewhat suspect. In particular, this effective dispersion relation may not be well-defined here because of the very presence of these higher derivative terms which produced the simplification in the final step. Further in these higher derivative contributions, the asymptotic behaviour of the factor $f''(r)+\frac{2}{r}f'(r)\sim(r_0/r)^6$ gives a very rapid decay and so perhaps modes propagating very close to the AdS boundary can evade our previous conclusion.

To eliminate these potential loopholes, we now proceed with a more careful analysis by rewriting the equation of motion (5.11) in a Schrödinger form, following [15, 17]. The first step is to isolate the ω^2 contributions by rewriting eq. (5.11) as

$$A(\rho,\mathfrak{q}^2)\,\partial_\rho^2\phi(\rho)+B(\rho,\mathfrak{q}^2)\,\partial_\rho\phi(\rho)+C(\rho,\mathfrak{q}^2)\,\phi(\rho)+D(\rho,\mathfrak{q}^2)\,\mathfrak{w}^2\phi(\rho)=0\,.\tag{5.16}$$

Here we have defined the dimensionless frequency and momentum,

$$\mathfrak{w}=\frac{\omega}{2\pi T}\,,\qquad \mathfrak{q}=\frac{q}{2\pi T}\,.\tag{5.17}$$

Performing a change of coordinates and rescaling $\phi(\rho)=Z(\rho)\psi(\rho)$ according to

$$\frac{dy}{d\rho}=\sqrt{\frac{D(\rho,\mathfrak{q}^2)}{A(\rho,\mathfrak{q}^2)}}\,,\qquad \frac{\partial_\rho Z(\rho,\mathfrak{q}^2)}{Z(\rho,\mathfrak{q}^2)}=\frac{\partial_\rho A(\rho,\mathfrak{q}^2)}{4\,A(\rho,\mathfrak{q}^2)}-\frac{\partial_\rho D(\rho,\mathfrak{q}^2)}{4\,D(\rho,\mathfrak{q}^2)}-\frac{B(\rho,\mathfrak{q}^2)}{2\,A(\rho,\mathfrak{q}^2)}\,,\tag{5.18}$$

the eq. (5.16) takes the desired form

$$-\frac{1}{\mathfrak{q}^2}\,\partial_y^2\psi(y)+\mathrm{U}(\mathrm{y},\mathfrak{q}^2)\,\psi(\mathrm{y})=\alpha^2\,\psi(\mathrm{y})\,,\tag{5.19}$$

JHEP08(2010)035

where $\alpha^2 = \mathfrak{w}^2/\mathfrak{q}^2$. Note that in terms of the Schrödinger coordinate y, the horizon now appears at $y \to +\infty$ and the asymptotic AdS boundary, at $y = 0$. In terms of the radial coordinate ρ, the effective potential can be expressed as

$$\mathfrak{q}^2 \mathrm{U}(\rho, \mathfrak{q}^2) = -\frac{\mathrm{A}(\rho, \mathfrak{q}^2)}{\mathrm{D}(\rho, \mathfrak{q}^2)} \frac{\partial_\rho^2 \mathrm{Z}(\rho, \mathfrak{q}^2)}{\mathrm{Z}(\rho, \mathfrak{q}^2)} - \frac{\mathrm{B}(\rho, \mathfrak{q}^2)}{\mathrm{D}(\rho, \mathfrak{q}^2)} \frac{\partial_\rho \mathrm{Z}(\rho, \mathfrak{q}^2)}{\mathrm{Z}(\rho, \mathfrak{q}^2)} - \frac{\mathrm{C}(\rho, \mathfrak{q}^2)}{\mathrm{D}(\rho, \mathfrak{q}^2)} \,. \tag{5.20}$$

More concretely the effective potential is of the form,

$$\mathfrak{q}^2 \mathrm{U}(\rho, \mathfrak{q}^2) = \frac{\sum_{\mathrm{i}=0}^{\mathrm{i}=6} \mathrm{n_i(u)} (\mathfrak{q}^2)^{\mathrm{i}}}{\sum_{\mathrm{i}=0}^{\mathrm{i}=5} \mathrm{d_i(u)} (\mathfrak{q}^2)^{\mathrm{i}}} \tag{5.21}$$

for some complicated functions n_i and d_i. If we now take the large momentum limit we obtain the result

$$\mathrm{U}(\rho, \mathfrak{q}^2) = \frac{\mathrm{f}(\rho)}{\mathrm{f}_\infty} + \mathcal{O}(1/\mathfrak{q}^2) \,. \tag{5.22}$$

Now this is precisely the effective potential which one would obtain for Einstein gravity in the large momentum limit. There is an infinite series of subleading corrections in $\mathcal{O}(1/\mathfrak{q}^2)$ which differ from Einstein theory but these terms are irrelevant in the limit of large $\mathfrak{q}$. This confirms our conclusion from the original analysis of the effective dispersion relation.

Notice that in principle one has to worry that the boundary and large momentum limits do not commute. This is clear from the form of expression (5.21), where the momentum appears in ratios. We will briefly comment on this in the discussion section. So perhaps a more subtle analysis may still find new constraints from demanding causality is respected in the dual CFT.

Our discussion here has focused on the tensor modes (5.10). However, the subtleties regarding the boundary and large q limits carry over to the vector and scalar channels. In the large q limit, one obtains the same results as in the tensor channel. That is, in this limit the higher momentum terms dominate and one obtains a trivial dispersion relation, leading to no causality violation. Now one may wish to apply a more careful analysis for these modes, along the lines of that given above for the tensor channel. However, unfortunately for the vector and scalar channels, the previous analysis with an effective Schrödinger equation can not be applied in a straightforward way because of the appearance of higher powers of $\mathfrak{w}$.

6 Holographic hydrodynamics

In this section, we compute the ratio of the shear viscosity to entropy density for five-dimensional quasi-topological gravity. By now, the holographic calculation of the shear viscosity is well understood. The first computations of this transport coefficient from an AdS/CFT perspective appeared in [3, 4] for Einstein gravity. These calculations were soon after extended to include higher curvature corrections to Einstein gravity, the first of example being the computation of the leading corrections to η/s for the strongly coupled $\mathcal{N} = 4$ super-Yang-Mills theory [6, 7, 9]. These computations were carried out for GB gravity [16, 18–23] and also higher order Lovelock theories [27–30], where the higher derivative terms need not be treated as small corrections. Further investigations also provided increasingly efficient techniques for these calculations [60–63] In the following, we will use the 'pole method' of [63].

JHEP08(2010)035

We begin with the metric for the planar AdS black hole given in eq. (2.6) and which we write out again here

$$\mathrm{d}s^2 = \frac{r^2}{L^2}\left(-\frac{f(r)}{f_\infty}\,\mathrm{d}t^2 + \mathrm{d}x^2 + \mathrm{d}x_2^2 + \mathrm{d}x_3^2\right) + \frac{L^2}{r^2 f(r)}\,\mathrm{d}r^2\,. \tag{6.1}$$

Recall that $f(r)$ is determined by roots of the cubic equation in eq. (2.7). Now it is convenient to transform to a radial coordinate $z = 1 - r_0^2/r^2$, with which the horizon is positioned at $z = 0$ and the asymptotic boundary, at $z = 1$. The metric then becomes

$$\mathrm{d}s^2 = \frac{r_0^2}{L^2(1-z)}\left(-\frac{f(z)}{f_\infty}\,\mathrm{d}t^2 + \mathrm{d}x_1^2 + \mathrm{d}x_2^2 + \mathrm{d}x_3^2\right) + \frac{L^2}{4f(z)}\,\frac{\mathrm{d}z^2}{(1-z)^2}\,. \tag{6.2}$$

An important feature of these coordinates is that $f(z)$ has a simple zero at the horizon. A Taylor expansion around $z = 0$ yields

$$f(z) = f_0'\,z + \frac{1}{2}\,f_0''\,z^2 + \frac{1}{6}\,f_0'''\,z^3 + \cdots\,, \tag{6.3}$$

where, e.g., $f_0' = \partial_z f|_{z=0}$. We present eq. (6.3) to establish a useful notation for the following.

Following [63], we perturb the metric (6.2) by shifting

$$dx \to dx + \varepsilon\, e^{-i\omega t}\, dy\,, \tag{6.4}$$

where ε is treated as an infinitesimal parameter. Then we evaluate the Lagrangian density, i.e., the entire integrand in eq. (2.1) including $\sqrt{-g}$, on the shifted background to quadratic order in ε. The presence of this off-shell perturbation (6.4) produces a pole at $z = 0$ in the (otherwise) on-shell action. The shear viscosity is then given by the 'time' formula [63]

$$\eta = -8\pi T \lim_{\omega,\varepsilon\to 0} \frac{\mathrm{Res}_{z=0}\,\mathcal{L}}{\omega^2\,\varepsilon^2}\,, \tag{6.5}$$

where $\mathrm{Res}_{z=0}\,\mathcal{L}$ denotes the residue of the pole in the Lagrangian density. Recall the Hawking temperature for the above black hole metric (6.2) is given in eq. (2.8). The final result of this calculation for quasi-topological gravity is

$$\eta = \frac{r_0^3}{2\ell_{\mathrm{P}}^3 L^3}\left[1 - 2\lambda f_0' - 9\mu\left(f_0'^2 + 2f_0''^2 + 2f_0'\left(f_0''' - 3f_0''\right)\right)\right]. \tag{6.6}$$

Now with the z coordinate, the cubic equation determining f can be written

$$f(z) - \lambda f(z)^2 - \mu f(z)^3 = z\,(2-z) \tag{6.7}$$

and substituting in the Taylor expansion (6.3), we can explicitly determine the coefficients:

$$f_0' = 2\,, \qquad f_0'' = -2(1-4\lambda)\,, \qquad f_0''' = -24(\lambda - 4\lambda^2 - 2\mu)\,. \tag{6.8}$$

The above expression (6.6) for the shear viscosity then becomes

$$\eta = \frac{r_0^3}{2\ell_{\mathrm{P}}^3}\left[1 - 4\lambda - 36\mu(9 - 64\lambda + 128\lambda^2 + 48\mu)\right]. \tag{6.9}$$

JHEP08(2010)035

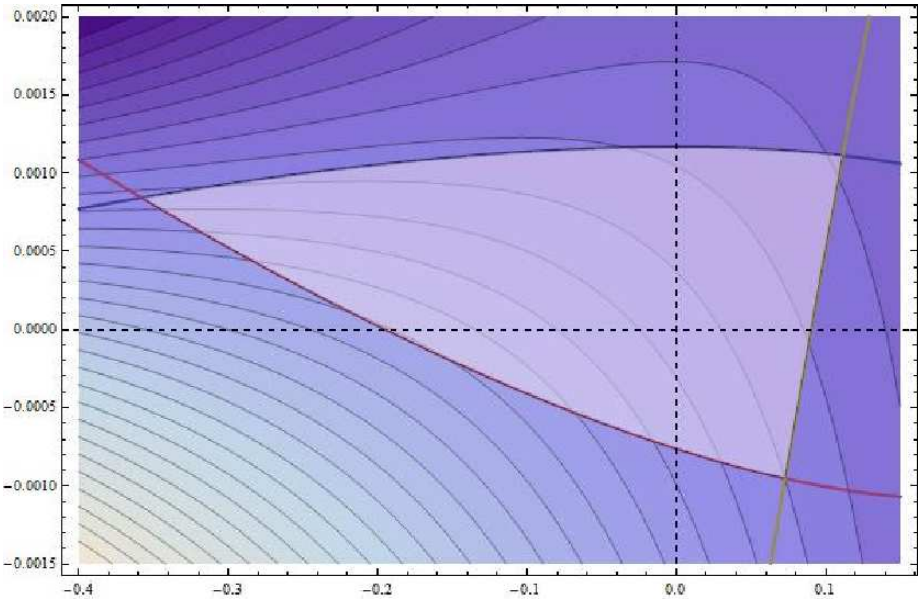

Figure 2. Contours of constant η/s shown in the allowed region of the gravitational couplings — see figure 1. The ratio increases in going from the lower-left to the upper-right in the plot.

We readily verify that with $\mu = 0$, this result (6.9) reduces to the expected result for GB gravity [16]. Combining this result with eq. (2.9), we find

$$\frac{\eta}{s} = \frac{1}{4\pi}\left[1 - 4\lambda - 36\mu(9 - 64\lambda + 128\lambda^2 + 48\mu)\right] . \tag{6.10}$$

A contour plot of the ratio of the shear viscosity to the entropy density in space of gravitational couplings, λ and μ, is shown in figure 2. From this plot, it is evident that η/s is maximized in the upper-right corner of the the allowed region of couplings. This point corresponds to the intersection of the boundaries defined by the tensor and vector constraints, i.e., eqs. (5.5) and (5.6), respectively. At this point, one finds

$$f_\infty = \frac{2838}{2543} , \quad \lambda = \frac{246671}{2684748} , \quad \mu = \frac{6466849}{5714486118} . \tag{6.11}$$

Hence we find the minimum value for η/s for the class of four-dimensional CFT's dual to quasi-topological gravity is

$$\frac{\eta}{s}\Big|_{\rm min} = \frac{347182615788747017}{838580510094780681}\,\frac{1}{4\pi} \simeq (.4140)\,\frac{1}{4\pi} . \tag{6.12}$$

Note that this point is well away from the region of instabilities which will be discussed in the next section. Hence we expect that our calculation of η/s at this point is reliable.

Within this class of CFT's, there is also a maximum value for η/s which appears to occur near the midpoint of the boundary produced by the scalar constraint (5.7). However, the point of the precise minimum lies in a region where, in the next section, we find that the uniform plasma is unstable — see figure 5. Hence our hydrodynamic calculations are not reliable at this precise point. Excluding the unstable region, it appears the maximum

JHEP08(2010)035

occurs very close to the point in GB gravity where η/s is maximized [18–20]. That is, the maximum is near $(\lambda, \mu) = (-1/8, 0)$ where we find

$$\frac{\eta}{s}\Big|_{\rm max} \simeq \frac{3}{2}\frac{1}{4\pi}\,. \tag{6.13}$$

7 Plasma Instabilities

Even when the various consistency conditions of section 5 are satisfied, there remains the possibility that the black hole solution is unstable. The dual statement would be that an infinite uniform plasma is an unstable configuration for the CFT. Such an instability need not represent a fundamental pathology of the CFT but rather indicate that some interesting new dynamics arises in CFT plasma for certain values of the couplings. However, it is still important to identify such instabilities as they would invalidate the assumption of local thermodynamic equilibrium and for example, discredit the results of our hydrodynamic calculations in section 6.

The appearance of such instabilities for five-dimensional GB theory were first noted in [16, 17]. Although causality or positive flux constraints allow the GB coupling to be in the range $-7/36 \leq \lambda \leq 9/100$, one finds that for $\lambda < -1/8$ a new instability arises. Evidence for the latter was given as follows: First one writes the equation of motion for the tensor modes in an effective Schrödinger form, as was done in section 5.3 above. For $\lambda < -1/8$, the potential develops a small well where $U < 0$ just in front of the horizon (i.e., near $\rho = 1$). For sufficiently large $\mathfrak{q}$, this well will support negative energy bound states which then correspond to unstable quasinormal modes, as described in [64]. Given that $\mathfrak{q}$ is finite (and large), this instability indicates that the uniform plasma becomes unstable with respect to certain non-uniform perturbations. On the gravitational side then, this instability seems similar in certain respects to the Gregory-Laflamme instability for black strings [65]. However, while the latter involves long wavelength modes, here the 'plasma instatiblity' occurs for arbitrarily short wavelengths. Examining the sound and shear channels, one finds that no additional instabilities arise in the consistent range, $-7/36 \leq \lambda \leq 9/100$ [17]. The same analysis has also been extended to GB gravity in higher dimensions [20]. For $D = 6$, one finds similar range where the theory passes all the known consistency tests but the uniform plasma is unstable. However, for $D \geq 7$, all of the potential instabilities are pushed outside of the allowed range of the GB coupling.

In this section, we will provide a preliminary investigation of potential plasma instabilities for five-dimensional quasi-topological gravity. Following the discussion above, our strategy will be to examine the tensor modes in detail using the effective Schrödinger equation, which was presented in eq. (5.19). As described previously, because of the appearance of higher powers of $\mathfrak{w}$ in the sound and shear mode equations, one cannot construct an effective Schrödinger problem in these cases. Hence a more elaborate analysis of the quasinormal modes would be required to detect instabilities in these channels.

We will separate our analysis into several different regimes, as we will find the behaviour of the theory will be quite different depending on the the sign of μ and the magnitude of

JHEP08(2010)035

$\mathfrak{q}^2$. To see this, consider eq. (5.16). In particular, let us examine the coefficients $A(\rho, \mathfrak{q}^2)$ and $D(\rho, \mathfrak{q}^2)$:

$$A(\rho,\mathfrak{q}^2) = -\rho^2 \frac{d}{d\rho}\left[\frac{1}{\rho}\left(1-2\lambda f(\rho)-3\mu f(\rho)^2\right)\right. \\ \left. +9\mu\,\rho\,\frac{d}{d\rho}\left(\rho f'(\rho)^2\right)-12\mu\frac{\mathfrak{q}^2}{f_\infty}\left(f(\rho)-2\rho f'(\rho)\right)\right], \tag{7.1}$$

$$D(\rho,\mathfrak{q}^2) = \frac{A(\rho,\mathfrak{q}^2)}{\rho\, f(\rho)^2} - 9\mu\frac{\rho}{f(\rho)}\left(9f'(\rho)+16\rho\, f^{(3)}(\rho)+4\rho^2\, f^{(4)}(\rho)\right). \tag{7.2}$$

The presence of the term proportional to $\mu\,\mathfrak{q}^2$ in the first expression creates the possibility that A (or D) may vanish, which we will see leads to a singularity in the Schrödinger potential. To see how this zero comes about, we first evaluate these functions at the horizon (i.e., $\rho = 1$). Using eq. (2.7), the polynomial defining $f(\rho)$, and $\rho = r_0^2/r^2$, we find

$$f(\rho) \simeq -2(\rho-1) - (1-4\lambda)(\rho-1)^2 + \cdots . \tag{7.3}$$

With this result, we find the corresponding expansions of A and D at the horizon

$$A \simeq A_0 + \mathcal{O}(\rho-1)\,, \qquad D = \frac{A_0}{4(\rho-1)^2} + \mathcal{O}(\rho-1) \tag{7.4}$$

with

$$A_0 = 24(3-8\lambda)\mu\,\frac{\mathfrak{q}^2}{f_\infty} + \left[1-4\lambda-36\mu(9-64\lambda+128\lambda^2+48\mu)\right]. \tag{7.5}$$

Hence we see that A vanishes at the horizon for a specific critical value of $\mathfrak{q}^2$:

$$\mathfrak{q}_c^2 = \frac{1-4\lambda-36\mu(9-64\lambda+128\lambda^2+48\mu)}{24(3-8\lambda)(-\mu)}\,. \tag{7.6}$$

Now comparing with eq. (6.10), we see the expression in the numerator above is precisely $4\pi\eta/s$. In the physically allowed region found in section 5.2, this ratio is always positive, as is the factor $3-8\lambda$ — see figure 1. Therefore we only have a valid solution for $\mathfrak{q}_c$ when μ is negative.

Note that A_0 vanishes when $\mathfrak{q} = \mathfrak{q}_c$ and so from eq. (7.4), both A and D vanish on the horizon at this point. For larger values of $\mathfrak{q}$, both A and D have a zero outside of the horizon (i.e., $\rho < 1$) but the two zeros appear at different radii.

From the above discussion, it is clear that we should separate the analysis into three distinct regimes: i) $\mu > 0$, ii) $\mu < 0$ and $|\mathfrak{q}| \leq \mathfrak{q}_c$ and iii) $\mu < 0$ and $|\mathfrak{q}| > \mathfrak{q}_c$.

7.1 Positive μ

In the case where $\mu \geq 0$, the functions A and D are positive everywhere outside of the horizon. Hence, the effective Schrödinger potential (5.20) is well behaved everywhere in the range of interest, $0 \leq \rho \leq 1$. To identify instabilities, it may seem that we can apply directly the strategy described above for GB theory of looking for a small negative dip in the effective potential just outside the horizon [16, 17, 20]. However, there is a small subtlety

JHEP08(2010)035

which requires a more detailed investigation for quasi-topological gravity. For GB gravity, one further considers the limit of large $\mathfrak{q}$, which corresponds to the limit of $\hbar \to 0$ from the point of view of the effective Schrödinger problem. With this limit, any small negative dip will always lead to negative energy bound states as solutions to eq. (5.19) and hence the appearance of an instability [64]. However, as found in section 5.3, the structure of the potential strongly depend on the value of the momentum for quasi-topological gravity. Indeed, our analysis showed that for sufficiently large momentum the effective potential reduces to that of Einstein gravity, i.e., $U \simeq f(\rho)/f_\infty$, and so no unstable modes would appear in this limit. That is, if one starts near an unstable point in GB theory but now with a small positive μ, then generically the modes become more stable as the momentum is increased. Hence in general one will have to investigate the potential for finite values of $\mathfrak{q}$ to find any unstable modes.

Following the reasoning of [64], we will still identify the unstable quasinormal modes as negative energy bound states in the effective Schrödinger problem. For a moment, let us consider applying the Bohr-Sommerfeld quantization rule for a zero-energy bound state:

$$\mathfrak{q} \int_{\rho_0}^{1} d\rho \, \frac{dy}{d\rho} \sqrt{-\mathrm{U}(\rho, \mathfrak{q}^2)} = \left(n - \frac{1}{2}\right) \pi \,. \tag{7.7}$$

Here, we are assuming that the potential dips to below zero between the horizon at $\rho = 1$ and some lower turning point where $\mathrm{U}(\rho = \rho_0, \mathfrak{q}^2) = 0$. For the zero-energy state, the quantum number n would be a specific positive integer. More generally, if we were to evaluate the integral on the left-hand side, then the integer part of n on the right would count the number of negative energy bound states supported by the potential well. Hence our strategy here is to scan of the parameter space (λ, μ) for positive μ. At each point, we vary $\mathfrak{q}$ looking for a negative dip in the potential near horizon. If the dip becomes sufficiently deep to support a bound state (i.e., to satisfy eq. (7.7) with $n = 1$), we will take this to signal of an instability in the system.

As discussed above for GB gravity, it was found that instabilities appear for $\lambda \leq -1/8$. Hence we focussed our scan of parameters on small positive values of μ in this regime and our numerical results are presented in figure 3. We should explicitly say that we expect that our Bohr-Sommerfeld analysis gives a good guide as to the unstable parameter space but it is difficult to assess how accurate the boundary of this region is in figure 3. In this regard, it is reassuring that the numerical curve reaches the λ axis very close to $\lambda = -0.125$ which, as indicated above, is where previous analysis [16, 17] indicated that GB gravity should become unstable.

Note that the unstable region is very narrow just above the λ axis but the height of this region increases as λ becomes more negative. Intuitively, this behaviour arises because for GB gravity at $\mu = 0$, an infinitesimal negative dip first appears in the potential at $\lambda = -1/8$ and then becomes larger as λ is decreased further. An infinitesimal dip appears is sufficient to support negative energy states in GB gravity because $\mathfrak{q}$ can be taken arbitrarily large without effecting the effective potential. As discussed above, with nonvanishing μ, increasing the momentum makes the potential more stable or, in other words, decreases the size of dip in U. Hence one must balance this effect with the increase

JHEP08(2010)035

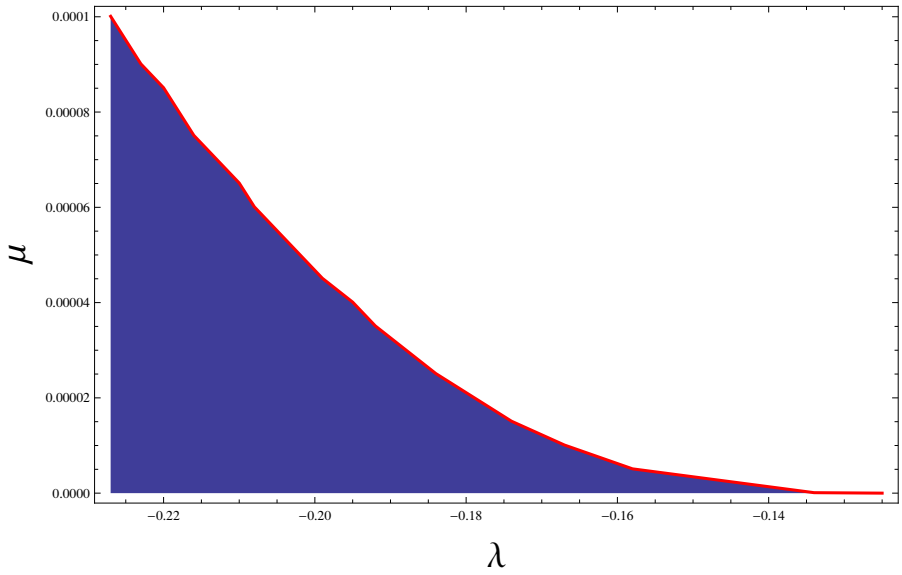

Figure 3. Instability boundary for the positive μ estimated using the Bohr-Sommerfeld analysis. The (blue) region below the (red) curve is unstable.

in the pre-factor $\mathfrak{q}$ in eq. (7.7). Therefore it is easier to find an instability for positive μ when when the initial size of the dip is larger at the corresponding point on the λ axis.

7.2 Negative μ and $|\mathfrak{q}| \leq \mathfrak{q}_c$

From our introductory discussion, we expect that the structure of the potential may be radically different for negative μ and particularly for $|\mathfrak{q}| \geq \mathfrak{q}_c$. Here we will examine the approach to the critical momentum, $\mathfrak{q} \to \mathfrak{q}_c$, and the same Bohr-Sommerfeld analysis as above will show that unstable modes occur over a large part of this parameter regime.

We are again looking for a negative potential well in front of the horizon, now for $\mu < 0$ and $|\mathfrak{q}| \leq \mathfrak{q}_c$. So to begin, consider the near horizon expansion of the effective potential (5.20):

$$\mathrm{U}(\rho, \mathfrak{q}^2) \simeq \frac{\mathrm{U}_0}{\mathrm{A}_0}(\rho - 1) + \frac{\mathrm{U}_1}{(\mathrm{A}_0)^2}(\rho - 1)^2 + \cdots , \tag{7.8}$$

where U_0 and U_1 are some constants and A_0 is given in eq. (7.5). An important point to notice is that as the momentum increases towards the critical value, $\mathfrak{q}^2 \to \mathfrak{q}_c^2$, we have $A_0 \ll 1$ and the above expansion becomes ill-defined. One must really perform a separate expansion for the special case $\mathfrak{q}^2 = \mathfrak{q}_c^2$, which yields

$$\mathrm{U}(\rho, \mathfrak{q}_c^2) \simeq \frac{1}{\mathfrak{q}_c^2}\frac{\mathrm{P}(\lambda, \mu)}{\mathrm{Q}(\lambda, \mu)} + \mathcal{O}(\rho - 1)\,. \tag{7.9}$$

where P and Q are polynomials in the couplings λ and μ. Their details are not important

JHEP08(2010)035

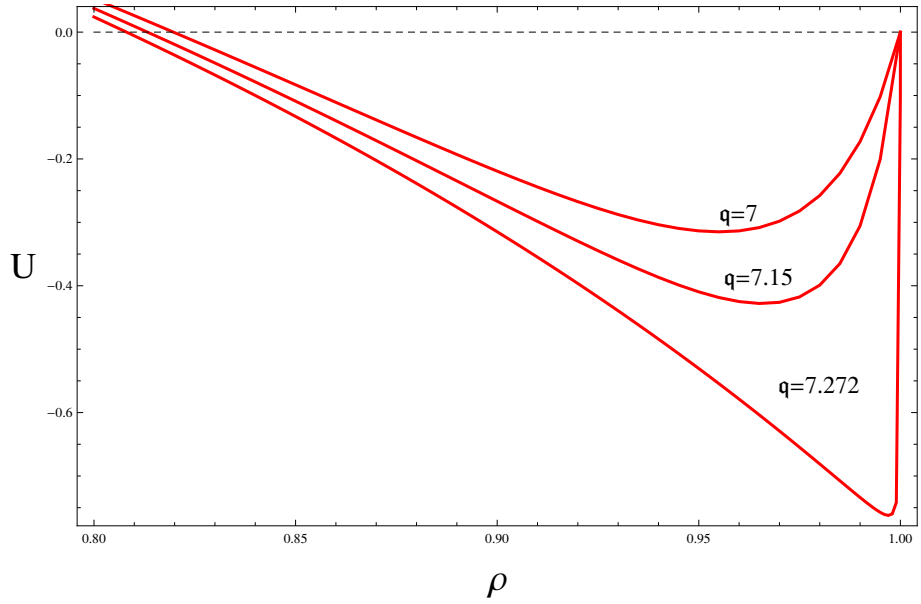

Figure 4. The effective Schrödinger potential in the tensor channel for $\mu = -0.0003, \lambda = -0.1$ and different values of $\mathfrak{q}^2$. Here $\mathfrak{q}_c \simeq 7.2725$. The effective potential at the horizon is tending to the constant value $P/(\mathfrak{q}_c^2 Q) \simeq -0.797$

but for completeness we present them here

$$\begin{aligned} P = {} & 2(1-4\lambda)^2\lambda + 3(-1+4\lambda)\left(-41+32\lambda\left(19-76\lambda+96\lambda^2\right)\right)\mu \\ & -36(1393+12\lambda(-1905+8\lambda(1469+176\lambda(-23+24\lambda))))\mu^2 \\ & -5184(161+24\lambda(-49+96\lambda))\mu^3 - 1990656\mu^4\,, \end{aligned} \tag{7.10}$$

$$\begin{aligned} Q = {} & 3(-1+4\lambda)(9+8\lambda(-5+8\lambda))\mu - 288\left(20+3\lambda\left(-189+16\lambda\left(97-310\lambda+336\lambda^2\right)\right)\right)\mu^2 \\ & -10368(-1+4\lambda)(-45+104\lambda)\mu^3 + 248832\mu^4\,. \end{aligned} \tag{7.11}$$

The essential result here is that while for $\mathfrak{q}^2 < \mathfrak{q}_c^2$, the effective potential went to zero on the horizon, precisely at the critical momentum, it is tending to a constant value at the horizon. Hence the limit $\mathfrak{q}^2 \to \mathfrak{q}_c^2$ is actually discontinuous. This unusual behaviour is illustrated with an example in figure 4.

The example in this figure also illustrates if this limiting constant value is negative, i.e., $\mathrm{U}(\rho = 1, \mathfrak{q}^2 = \mathfrak{q}_c^2) < 0$, then the effective potential develops a negative well in front of the horizon as we approach the critical momentum. Hence there is the possibility of developing instabilities in this regime. The dip in potential is largest with $\mathfrak{q}^2 = \mathfrak{q}_c^2$ and so we focus on this case. Once again, we will use the Bohr-Sommerfeld rule (7.7) to test for negative energy bound states. As before, we also have to worry that $A_0 \to 0$ as $\mathfrak{q}^2 \to \mathfrak{q}_c^2$ and so we must perform a separate expansion to evaluate $dy/d\rho$ at this point

$$\frac{dy}{d\rho} \simeq -\frac{j_0}{2(\rho-1)} + \cdots\,, \qquad \text{where } j_0 = \sqrt{\frac{3\mu\, Q(\lambda,\mu)}{R(\lambda,\mu)}}\,, \tag{7.12}$$

JHEP08(2010)035

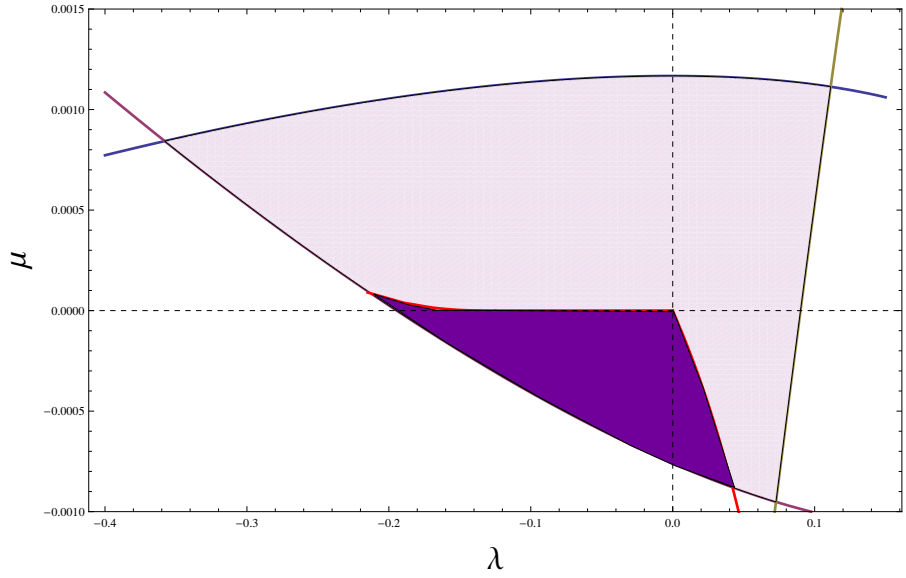

Figure 5. Unstable region (purple) for the tensor channel combining the results of sections 7.1 and 7.2, superimposed onto the region (pink) allowed by positivity of energy flux. In the section 7.3, the analysis is extended to $|\mathfrak{q}| > \mathfrak{q}_c$ and it appears instabilities are present throughout the entire $\mu < 0$ region.

where Q was given above in eq. (7.11) and

$$R = 3\mu Q + 108\,\mu\,(1-4\lambda)(3-8\lambda)\,(3-80\lambda(1-4\lambda)+320\mu)\ . \tag{7.13}$$

Hence the Bohr-Sommerfeld integral (7.7) yields an expression of the form

$$\left(n-\frac{1}{2}\right)\pi \simeq \frac{1}{2}\int_1^{\rho_0} d\rho \left(\frac{1}{\rho-1}\sqrt{\frac{-3\mu\,P}{R}}+\cdots\right)\ . \tag{7.14}$$

This integral produces logarithmic divergence indicating that there are an infinite number of unstable modes in this limit. Of course, this result is only true at strictly $\mathfrak{q} = \mathfrak{q}_c$. However, by taking the momentum arbitrarily close to the critical value, the resulting negative dip in the potential will always support a large number of unstable modes as well.

To summarize, we must exclude as unstable the region with $\mu < 0$ where the effective potential tends to a negative constant on the horizon at the critical value $\mathfrak{q}_c$. That is, the region where $\mu < 0$ and $P/Q \leq 0$. The boundary of this region is well approximated by the curve

$$\mu \simeq -\frac{2}{123}\,\lambda - \frac{14120}{206763}\,\lambda^2 - \frac{27472807424}{28153056843}\,\lambda^3. \tag{7.15}$$

Putting this constraint for negative μ together with that obtained for positive μ in the previous section, one obtains the unstable region shown in figure 5. Here we are showing the region of instability together with the physically allowed region defined by the constraints in eqs. (5.5)–(5.7).

JHEP08(2010)035

7.3 Negative μ and $|\mathfrak{q}| > \mathfrak{q}_c$

With $\mu < 0$, we are of course free to take the momentum beyond the critical value. As noted above, when $\mathfrak{q}^2 > \mathfrak{q}_c^2$, both A and D have a zero at some finite radius outside of the horizon but the two zeros appear at different radii. Let us label the two zeros as ρ_A and ρ_D. In the following, we consider the case where $\rho_A > \rho_D$, but in general this depends in detail on the values of λ and μ. However, the following analysis is easily adapted to the opposite situation where $\rho_A < \rho_D$ and the conclusions will be unchanged.

Let us first consider the effective potential in the vicinity of D's zero. Expanding the various coefficients in eq. (5.16) around $\rho \simeq \rho_D$ gives

$$\begin{aligned} A &= A_0 + \mathcal{O}\left(\rho - \rho_D\right) , \\ B &= B_0 + \mathcal{O}\left(\rho - \rho_D\right) , \\ C &= C_0 + \mathcal{O}\left(\rho - \rho_D\right) , \\ D &= -D_1(\rho - \rho_D) + \mathcal{O}\left((\rho - \rho_D)^2\right) . \end{aligned} \tag{7.16}$$

It is important to note that the constants A_0 and D_1 are both positive, so that $dy/d\rho$ in eq. (5.18) is well defined in the region $\rho < \rho_D$. Using the expressions above, along with eq. (5.18), we find

$$y_D - y \simeq \frac{2}{3}\sqrt{\frac{D_1}{A_0}}\,(\rho_D - \rho)^{3/2} \tag{7.17}$$

$$Z \simeq (\rho_D - \rho)^{-1/4} . \tag{7.18}$$

Finally, with eq. (5.20), we obtain the effective potential

$$\begin{aligned} \mathfrak{q}^2\,\mathrm{U}(\rho) &= -\frac{A_0}{D_1}\,\frac{5/16}{(\rho - \rho_D)^3} \\ &= -\frac{5/36}{(y_D - y)^2} . \end{aligned} \tag{7.19}$$

Hence we find that the effective potential contains a singularity at $\rho = \rho_D$ but the structure of the singularity is surprisingly simple. In particular, the coefficient is completely independent of the parameters, λ, μ and $\mathfrak{q}$, but of course, the latter still determine the precise location of the singularity.

We can perform a similar analysis for the effective potential in the vicinity of the zero in A. We begin by expanding around $\rho \simeq \rho_A$

$$\begin{aligned} A &= -A_1\left(\rho - \rho_A\right) + \mathcal{O}\left((\rho - \rho_D)^2\right) , \\ B &= -A_1 + \mathcal{O}\left(\rho - \rho_A\right) , \\ C &= \hat{C}_0 + \mathcal{O}\left(\rho - \rho_A\right) , \\ D &= -D_0 + \mathcal{O}\left(\rho - \rho_A\right) . \end{aligned} \tag{7.20}$$

JHEP08(2010)035

for some positive constants D_0 and A_1. Note that the leading coefficient in B has the special form $B_0 = A_1$, which follows from the original equation (5.11). Then in this case

$$y - y_A \simeq 2\sqrt{\frac{D_0}{A_1}}\,(\rho - \rho_A)^{1/2}\,, \tag{7.21}$$

$$Z \simeq (\rho - \rho_A)^{-1/4} \tag{7.22}$$

and the potential becomes

$$\begin{aligned} \mathfrak{q}^2\,\mathrm{U}(\rho) &= -\frac{A_1}{D_0}\,\frac{1/16}{\rho - \rho_A} \\ &= -\frac{1/4}{(y - y_A)^2}\,. \end{aligned} \tag{7.23}$$

Here again we find that the effective potential contains a singularity with a very simple form at the zero of A. The parameters, λ, μ and $\mathfrak{q}$, fix the precise location of the singularity but the overall coefficient is independent of these.

Implicitly the above analysis assumes that $\rho > \rho_A$ where both A and D are negative. Similarly in consider the zero in D, we assumed $\rho < \rho_D$ where both A and D are positive. Special consideration must be given to the range $\rho_D < \rho < \rho_A$ where $D < 0$ and $A > 0$. To accommodate the latter, we must modify the construction of the effective Schrödinger equation (5.19) slightly. In particular, in eq. (5.18), the definition of the new coordinate is replaced by

$$\frac{dy}{d\rho} = \sqrt{-\frac{D(\rho, \mathfrak{q}^2)}{A(\rho, \mathfrak{q}^2)}}\,. \tag{7.24}$$

The final result can then be most simply expressed as flipping the sign of both the effective potential and the effective energy of eq. (5.19). That is, in this region, the Schrödinger equation becomes

$$-\frac{1}{\mathfrak{q}^2}\,\partial_y^2\psi(y) + \left[-\mathrm{U}(\mathrm{y}, \mathfrak{q}^2)\right]\,\psi(y) = \left[-\alpha^2\right]\,\psi(y)\,, \tag{7.25}$$

where U is given by precisely the same expression in eq. (5.20) and $\alpha^2 = \mathfrak{w}^2/\mathfrak{q}^2$, as before. For present purposes, the behaviour near the zeros $\rho = \rho_D$ and ρ_A are of primary interest. Carefully keeping track of the signs, one finds that near these points, the Schrödinger equation (7.25) has precisely the same form as above, with a singular and attractive potential. That is, in the vicinity of these zeros, we may write the Schrödinger equation as

$$-\psi''(y) - \frac{\gamma}{y^2}\,\psi(y) \simeq 0 \tag{7.26}$$

where $\gamma = 5/36$ for $\rho = \rho_D$ and $1/4$ for $\rho = \rho_A$. In either case we have shifted the y coordinate to put the singularity at the origin. The $1/y^2$ potential has been studied extensively in the literature [66–69]. Remarkably for a one-dimensional Schrödinger equation, the value $\gamma = 1/4$ marks the boundary between the conformal regime when the potential is repulsive or weakly attractive and the regime with a sufficiently attractive potential where discrete bound states appear and conformality is lost.

JHEP08(2010)035

The key point in presenting eq. (7.26) that this equation applies here for both positive and negative y. However, in this one-dimensional setting, the wave-function must propagate through the singularity at $y = 0$. So one should approach the problem by solving for $y < 0$ and $y > 0$ independently and then matching the solutions with an appropriate boundary condition at the origin. This procedure is most easily demonstrated for the zero in D, in which case $\gamma = 5/36$. Then eq. (7.26) has two independent solutions

$$\begin{aligned} \psi(y) &= d_1\, y^{1/6} + d_2\, y^{5/6} && \text{for} \quad y > 0\,, \\ \psi(y) &= \tilde{d}_1\, (-y)^{1/6} + \tilde{d}_2\, (-y)^{5/6} && \text{for} \quad y < 0\,. \end{aligned}$$

Using eqs. (7.17) and (7.18) above, we can convert these back to the radial profile of the original tensor mode, i.e., $\phi = Z\psi$, in the vicinity $\rho \simeq \rho_D$

$$\begin{aligned} \phi(\rho) &= \delta_1 + \delta_2(\rho - \rho_D) && \text{for} \quad \rho < \rho_D\,, \\ &= \tilde{\delta}_1 + \tilde{\delta}_2(\rho - \rho_D) && \text{for} \quad \rho > \rho_D\,. \end{aligned} \tag{7.27}$$

Matching of solutions at ρ_D is achieved straightforwardly by imposing continuity of the radial profile and its first derivative, i.e., $\delta_1 = \tilde{\delta}_1$ and $\delta_2 = \tilde{\delta}_2$. Hence while some care must be taken, the zero in D presents no real difficulty in finding well-behaved solutions.

Next we turn to the zero in A, where the situation is more subtle. In this case, $\gamma = 1/4$ in eq. (7.26) and the two independent solutions are

$$\begin{aligned} \psi(y) &= a_1\, y^{1/2} + a_2\, y^{1/2}\, \log(y) && \text{for} \quad y > 0\,, \\ \psi(y) &= \tilde{a}_1\, (-y)^{1/2} + \tilde{a}_2\, (-y)^{1/2}\, \log(-y) && \text{for} \quad y < 0\,. \end{aligned}$$

Using eqs. (7.21) and (7.22), these expressions are translated to the radial profile $\phi = Z\psi$ in the vicinity $\rho \simeq \rho_A$

$$\begin{aligned} \phi(\rho) &= \alpha_1 + \alpha_2 \log(\rho - \rho_A), && \text{for} \quad \rho > \rho_A\,, \\ &= \tilde{\alpha}_1 + \tilde{\alpha}_2 \log(\rho_A - \rho), && \text{for} \quad \rho < \rho_A\,. \end{aligned} \tag{7.28}$$

The matching at ρ_A is slightly more involved because of the logarithmic behaviour of these solutions. Integrating the equation of motion (5.16) around ρ_A, we obtain

$$-\,A_1(\rho - \rho_A)\partial_\rho\phi\big|_{\rho_A-\epsilon}^{\rho_A+\epsilon} = \int_{\rho_A-\epsilon}^{\rho_A+\epsilon} d\rho\, \left(D_0\, \mathfrak{w}^2 - \hat{C}_0\right) \phi\,. \tag{7.29}$$

As $\epsilon \to 0$, the right-hand side vanishes and the vanishing of the left-hand side requires $\alpha_2 + \tilde{\alpha}_2 = 0$. Another natural boundary condition is that the flux of probability in the effective Schrödinger problem should be continuous as the wave-function propagates through the singularity at $y = 0$. If we express this flux in terms of the radial profile ϕ and the coordinate ρ, then we require

$$\mathrm{Im}\big[\phi^* A_1(\rho - \rho_A)\partial_\rho\phi\big]_{\rho_A-\epsilon}^{\rho_A+\epsilon} = 0\,.$$

JHEP08(2010)035

Continuity then leads to $\mathrm{Im}(\alpha_1^* \alpha_2) = \mathrm{Im}(\tilde{\alpha}_1^* \tilde{\alpha}_2)$ and so it seems natural to set $\alpha_1 = -\tilde{\alpha}_1$ as well.[5] Our final solution in the vicinity of $\rho \simeq \rho_A$ then takes the form

$$\phi = (\alpha_1 + \alpha_2 \log|\rho - \rho_A|)\ \mathrm{sgn}(\rho - \rho_A)\,. \tag{7.30}$$

Again the constants α_1 and α_2 are arbitrary but our analysis shows appropriate boundary conditions at this point will produce a suitable physical solution.

At this stage, we have shown that despite of the appearance of new singularities in the equation of motion (5.16) in this regime (i.e., $\mu < 0$ and $|\mathfrak{q}| > \mathfrak{q}_c$), we may more or less straightforwardly solve for the radial profile ϕ. The precise solutions and the corresponding quasinormal eigenfrequencies $\mathfrak{w}$ will still be set by the boundary conditions on the field at the black hole horizon $\rho = 1$ and at the asymptotic boundary $\rho = 0$. To better understand these boundary conditions, we now return to the overall behaviour of the effective Schrödinger potential.

Figure 6 provides an example of the effective potential in the desired regime. One point which the figure illustrates is that for large momenta $\mathfrak{q}^2 \gg \mathfrak{q}_c^2$, the general discussion of section 5.3 still applies here and over most of the range the effective potential approaches that of Einstein gravity, i.e., $U \simeq f(\rho)/f_\infty$. However, the figure also makes evident the singularities extensively discussed above, which appear as sharp dip at $\rho = \rho_A$ and ρ_D. As is typical of $\mathfrak{q}^2 \gg \mathfrak{q}_c^2$, the zeros are very close together and in fact it is difficult to resolve the two distinct singularities in the example given in figure 6. Intuitively, one expects that this deviation of the Einstein potential will provide a small perturbation and so there will be a set of stable modes whose quasinormal frequencies and radial profiles deviate only slightly from the solutions in Einstein gravity.

However, the singularities introduce a new boundary surface into the problem and we argue that this also leads to a additional set of new unstable modes, as follows: The Einstein potential vanishes at the horizon and so solving the Schrödinger equation (5.19) with a negative energy yields two independent solutions, one which grows exponentially (and diverges at the horizon) and another which decays. Similarly, there are two asymptotic solutions, one which grows and another which decays as one approaches the AdS boundary. Now the potential is smooth throughout $0 < \rho < 1$ if we are considering pure Einstein gravity. As a result, the solution which decays at the horizon is precisely that which grows at the asymptotic boundary and vice versa. Hence one finds no normalizable solutions with a negative effective energy which agrees with the result that the black hole is stable in Einstein gravity. However, if we consider quasi-topological gravity with $\mu < 0$ and $|\mathfrak{q}| > \mathfrak{q}_c$, while the effective potential is well approximated by the Einstein potential for most radii, a dramatic difference arises with the appearance of the singularities at $\rho = \rho_A$ and ρ_D. Now we have the possibility of matching a solution in the range $\rho > \rho_A$ which decays at the horizon to a solution in the range $\rho < \rho_D$ which decays at the asymptotic boundary. Because of the sign of the effective energy in the Schrödinger equation (7.25) is flipped in the range $\rho_D < \rho < \rho_A$, the solution would be oscillatory in this interval

[5] This is not a unique solution for this constraint and so it may be that a further boundary condition should be applied to single out this result as the unique physical solution.

JHEP08(2010)035

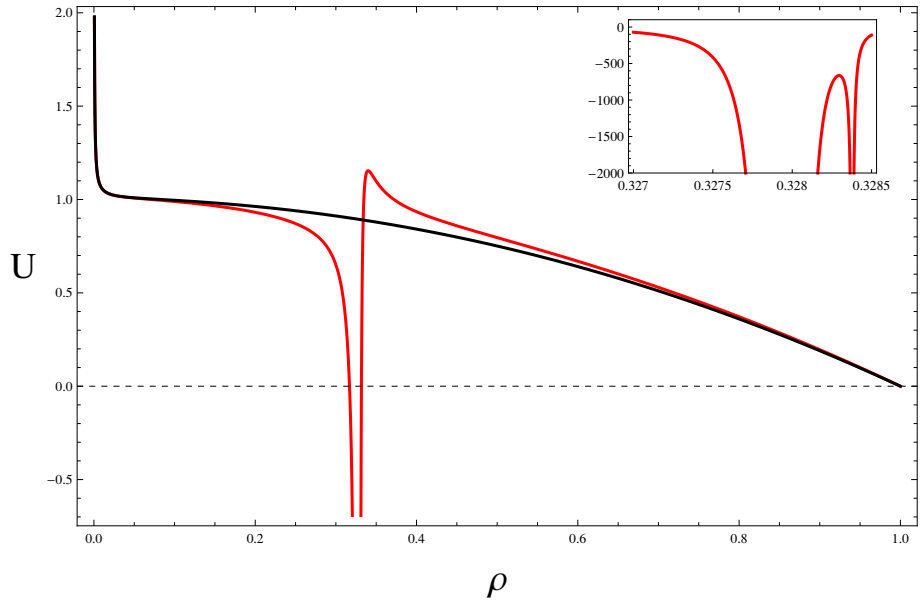

Figure 6. Comparison of the effective potential for $\mu < 0$ and $\mathfrak{q}^2 > \mathfrak{q}_c^2$ (red) with that for Einstein gravity (black). The red curve is given for $\lambda = -0.1$, $\mu = -0.0003$ and $\mathfrak{q} = 40$. For these gravitational couplings, the critical momentum is approximately $\mathfrak{q}_c \simeq 7.27$. The inset shows a close-up of the effective potential to resolve the two separate singularities at $\rho_A = 0.328378$ and $\rho_D = 0.327955$. (Note that in keeping with the discussion at eq. (7.25), the sign of U in the inset has been reversed on the interval $\rho_A > \rho > \rho_D$.)

and tuning α^2 should allow us to match onto the decaying solutions with the boundary conditions indicated above. Hence we should also be able to construct an infinite set of negative energy states which are localized near the interval $\rho_D < \rho < \rho_A$. It appears that these unstable modes would naturally be regarded as the progeny of the diverging number of unstable modes which were found to accumulate in the limit $\mathfrak{q}^2 \to \mathfrak{q}_c^2$, in the previous section. In any event, our conclusion is that generally when μ is negative, the black holes in quasitopological gravity have unstable quasinormal modes with $|\mathfrak{q}| > \mathfrak{q}_c$.

To summarize, our analysis in this section indicates that instabilities appear in the tensor channel throughout the lower half of the space of couplings with $\mu < 0$ and in the narrow sliver shown in figure 3 with $\mu > 0$. However, we should re-iterate that our analysis here only represents a preliminary investigation of the potential plasma instabilities in five-dimensional quasi-topological gravity. A thorough and detailed analysis of the quasinormal modes is required to validate the results derived here and to develop a full picture of the unstable modes.

8 Discussion

In this paper, we have begun an examination of the holographic properties of quasi-topological gravity. The main new feature of this toy model is that it allows us to examine CFT's in which the flux parameter t_4 in eq. (4.1) is nonvanishing. In this case, the dual

JHEP08(2010)035

CFT cannot be supersymmetric [13] and so these new models allow us to begin exploring holography in a context which is fundamentally nonsupersymmetric. In this regard, quasi-topological gravity differs from Lovelock theories which are consistent with supersymmetry [70]. Of course, conformal fixed points are believed to occur for a wide variety of nonsupersymmetric gauge theories [71–76]. Further one might speculate that extending some of these to large N_c and strong coupling may generate a holographic dual close to Einstein gravity [77–80]. Hence, in the spirit of exploring quasi-topological gravity as a toy model, one may gain new insights into such conformal fixed points.

One aspect of physics which we explored was the hydrodynamic properties of the CFT plasma. In particular, we calculated the ratio of shear viscosity to entropy density (6.10). Similar results have already been found in a framework where the curvature-cubed terms were treated perturbatively [51]. Eq. (6.10) should reduce to these results in the regime of small couplings where one only keeps the terms linear in λ and μ. Our full nonperturbative calculation is straightforward using the techniques developed in [63] and produces a final expression which contains contributions which are nonlinear in the gravitational couplings, e.g., proportional to $\mu\,\lambda^2$. This differs from cubic Lovelock theories in higher dimensions which also contain curvature cubed interactions. In fact, in this case, η/s is independent of the coupling constant controlling the curvature-cubed interactions [27–30, 81] and remains simply linear in the curvature squared coupling, as in GB gravity [16, 18–20]. Of course, these theories are also distinguished from the present case since t_4 remains zero in the Lovelock theories despite the appearance of the curvature cubed interaction [27–30].

Considering the value of η/s when $t_4 \neq 0$, we find no dramatic behaviour. The value smoothly increases or decreases as we move away from the axis into the (λ, μ) plane, as illustrated in figure 2. One point that this analysis makes clear is that $\eta/s = 1/4\pi$ is simply a codimension one surface (here a contour) which cuts through the space of gravitational couplings or alternatively through the space of parameters which differentiate the dual CFT's. The main feature that distinguishes this surface is that it runs through the point where the bulk theory is Einstein gravity, which we favour as theorists. This illustrates that even if η/s was found to be precisely $1/4\pi$ for some system arose in nature (e.g., the quark-gluon plasma or a trapped atomic gas), there is no guarantee that the holographic dual would anywhere be close to a theory of Einstein gravity.

This holographic model also illustrates the point that the CFT plasma can readily achieve $\eta/s < 1/4\pi$. Of course, even though the originally conjectured KSS bound on η/s has been proven incorrect, there are still general arguments to suggest that this ratio should satisfy some lower bound [3, 4, 37]. Hence the question naturally arises as to the precise nature of such a bound. Holographic models provide an excellent theoretical framework to study this question, as they provide access to a variety of strongly coupled fluids in this 'KSS regime' where η/s is unusually small.

In the present case of holographic fluids modeled by quasi-topological gravity, this ratio reaches a minimum value at the upper corner of the allowed parameter space with $\eta/s \simeq (0.4140)/(4\pi)$, as given in eq. (6.12). It may be of interest to note that at the point, the dual CFT has $t_2 = 0$ while t_4 reaches its maximal value with $t_4 = 15/2$. It is clear that this value does not represent a fundamental bound. If one explores holographic models

JHEP08(2010)035

with GB gravity in higher dimensions, one finds the minimum ratio is $\eta/s \simeq (0.4139)/(4\pi)$ for $D \simeq 9.207$ [18–20]. This analysis was also extended to Lovelock gravity with a cubic curvature interaction for $D \geq 7$ [27–30]. Initially here, it appeared that η/s could be pushed to zero (or even negative values) but taking care to account for plasma instabilities, one finds that the hyrdodynamic results are only reliable down to $\eta/s \sim (0.3938)/(4\pi)$ [82]. The cubic interaction of quasi-topological gravity can also be extended to higher $D \geq 7$ [36] and so it would be interesting to examine the contributions of such interactions to higher dimensional holographic models. One might note the Lovelock models introduce additional parameters to distinguish the dual CFT's but still have $t_4 = 0$. While it is perhaps not surprising then, these results explicitly demonstrate that many more parameters in the CFT will effect the value of η/s than simply $\mathcal{A}$, $\mathcal{B}$ and $\mathcal{C}$, the three couplings which fix the the three-point function of the stress tensor.

While the various holographic models above all seem to point to a minimum value around $\eta/s \sim (0.4)/(4\pi)$, it seems clear that this collection of models only explores a limited parameter space. One might imagine that one can continue to systematically lower η/s by continuing explore a wider range of CFT's by adding more and more interesting couplings in the dual gravitational theory (and without introducing any other pathologies in the holographic model). In fact, there seems to be some evidence in favour of such a scenario at least in very high dimensions [83].

There is one difference between quasi-topological gravity and GB gravity (or the more general Lovelock theories) which is particularly striking. All of the Lovelock gravity models are distinguished by having second order equations of motion while the general equations in quasi-topological gravity are fourth order. It seems that the latter is inevitable in order to produce a holographic theory where $t_4 \neq 0$ since the Lovelock theories are in fact the most general gravitational theories with second order equations of motion [84, 85]. To develop some intuition for such higher order equations, we might establish an analogy with a higher-derivative scalar field equation (in flat space)

$$\left(\Box + \frac{a}{M^2}\Box^2\right)\phi = 0\,. \tag{8.1}$$

Here we imagine M^2 is some high energy scale and a is the dimensionless coupling that controls the strength of the higher-derivative term. The (flat space) propagator for this scalar can be written as

$$\frac{1}{q^2(1 - a\,q^2/M^2)} = \frac{1}{q^2} - \frac{1}{q^2 - M^2/a}\,. \tag{8.2}$$

Now the $1/q^2$ pole is associated with the regular modes which are easily excited at low energies. The second pole $1/(q^2 - M^2/a)$ is associated with ghost modes that appear out at the high energy scale. Depending on the sign of a, these new modes may have a regular mass ($a < 0$) or be tachyonic ($a > 0$). Further writing out the dispersion relation for the ghost modes, we have

$$q^2 - M^2/a = -\omega^2 + (k^i)^2 - M^2/a = 0\,. \tag{8.3}$$

JHEP08(2010)035

As noted, when a is negative, the mass above has the 'right sign' and these modes only go on-shell when $\omega^2 \sim M^2/|a|$, i.e., at very high energies. On the other hand, if a is positive, the modes are 'unstable' and in this case, we can bring these modes on-shell above a certain threshold of large spatial momentum, i.e., $(k^i)^2 \sim M^2/a$. Comparing this discussion to our analysis of the tensor channel equation for quasi-topological gravity, the coupling μ for the curvature-cubed interactions would play a role analogous to a above. In parallel with the present scalar theory in section 7.3, we found that a new set of unstable modes appears above a certain momentum threshold for a particular sign of μ, i.e., $\mathfrak{q}^2 \geq \mathfrak{q}_c^2$ for $\mu < 0$.

One important point that arises in the scalar field model is that the extra high energy modes are ghosts for either sign of a, as seen from the overall sign of their contribution to the propagator (8.2). Hence a natural worry would be that ghosts must also appear in quasi-topological gravity but we will argue that this is not the case, in the following. In section 7, we have found new unstable modes in quasi-topological theory. This certainly indicates that working on the uniform black hole background is problematic but it is not clear that they indicate that there is a fundamental pathology in the form of ghost modes. One important difference between the equations in quasi-topological gravity and in the simple scalar model are that the former are not Lorentz invariant (in the gauge theory directions). Of course, the lack of Lorentz invariance is not a surprise since the black hole background is dual to a uniform finite temperature plasma which defines a preferred reference frame. Hence the same statement would apply even if we were considering graviton modes in a black hole solution of Einstein gravity. However, the discrepancy is more significant for the higher derivative terms here. For example, while a $\mathfrak{q}^4$ term appears in eq. (5.15) there is no $\mathfrak{w}^4$ contribution. Hence it is not clear whether the additional instabilities appearing in the black hole background are associated with ghost modes.

Let us consider this point further. At zero temperature, the background spacetime reduces to simply AdS_5 and as noted before with eq. (2.10), the linearized equations of motion reduce to the second order equations of Einstein gravity. Hence in this limit, both the higher derivative contributions and the additional unstable modes vanish for any values of λ and μ. As noted in [36], the higher derivative terms appear in the linearized equations of motion through couplings to the background curvature when one is considering fluctuations around a nontrivial background spacetime. In particular, these terms arise from a nontrivial Weyl curvature in the background, e.g., for a transverse traceless mode (i.e., $\nabla^a h_{ab} = 0$) and $h^a{}_a = 0$), the four-derivative terms can be written as [36]:[6]

$$C^{cdef}\, h_{de;cf(ab)} + 2\left(\Box h^c{}_{(a}\right)^{;de} C_{|cde|b)} + 2\,\Box^2 h^{cd} C_{cadb} + g_{ab}\,(\Box h_{cd})_{;ef}\, C^{cedf}\,. \tag{8.4}$$

Hence the specific features of any instabilities will always depend on the details of the background geometry under study. It may be of interest to explicitly repeat the analysis of section 7 for other nontrivial configurations, i.e., one simple example would be the confining phase represented by the AdS soliton [86].

Another interesting aspect of these higher derivative terms (8.4) is that they will vanish in the asymptotic region with AdS boundary conditions, since the Weyl curvature will vanish there. Hence any unstable modes associated with these terms will be 'confined' to the

[6]Here we adopt the standard notation: $T_{(ab)} = \frac{1}{2}\,(T_{ab} + T_{ba})$.

JHEP08(2010)035

interior, e.g., near the horizon. Hence in the dual CFT, the instabilities will be associated with dynamics of infrared excitations and will be insensitive to the ultraviolet details of the theory. Given this observation and the previous discussion, it seems then that these problems cannot represent a fundamental pathology, i.e., ghosts, in the theory. Hence we would conclude that the analogy with the scalar field in eq. (8.1) is simply deficient in this respect.

Still the higher derivative terms and the resulting instabilities are a worrying aspect of quasi-topological gravity. In particular, we have made a preliminary analysis of the shear and sound channel equations of motion. In this case, it appears that the coefficient analogous A in eq. (5.16) can again have go to zero but when μ is positive. Hence one would be tempted to conclude that instabilities will now appear for positive μ. Unfortunately, this would mean that the plasma is only stable with $\mu = 0$. This makes the need for a detailed analysis of the quasinormal modes even more pressing to develop a full picture of the instabilities.

To close, let us re-iterate that quasi-topological gravity was introduced as a toy model to study extensions of the usual AdS/CFT correspondence. We have not identified an approach by which the new gravitational action (2.1) emerges from a UV complete theory and we have no reason to expect that the new theory is radiatively stable. If one were tempted to construct a full quantum version of quasi-topological gravity, another issue which would need to be addressed is the appearance of several different vacua (corresponding to the roots of eq. (2.5)) and in particular vacua in which the graviton is a ghost. It is not clear what the role of these vacua would be in, e.g., a path integral formulation of the theory.[7] All of these considerations as well as the appearance of instabilities at large momenta reinforce the idea that quasi-topological gravity (as well as Lovelock theories of gravity) should only be treated as toy models which may give us insight into the long wavelength physics, e.g., hydrodynamic behaviour, of strongly coupled conformal fixed points.

Acknowledgments

It is a pleasure to thank Pavel Kovtun, Brandon Robinson, Dam Son and Andrei Starinets for useful correspondence and conversations. RCM would also like to thank the KITP and the Weizmann Institute for hospitality at various stages of this project. Research at the KITP is supported by the National Science Foundation under Grant No. PHY05-51164. Research at Perimeter Institute is supported by the Government of Canada through Industry Canada and by the Province of Ontario through the Ministry of Research & Innovation. RCM also acknowledges support from an NSERC Discovery grant and funding from the Canadian Institute for Advanced Research. MFP is supported by the Portuguese Fundacao para a Ciencia e Tecnologia, grant SFRH/BD/23438/2005. MFP would also like to thank the Perimeter Institute for hospitality at various stages of this project.

[7] A related issue was studied for Lovelock gravity in [87, 88] but found not to be problematic.

JHEP08(2010)035

References

[1] J.M. Maldacena, *The large-N limit of superconformal field theories and supergravity*, *Adv. Theor. Math. Phys.* **2** (1998) 231 [*Int. J. Theor. Phys.* **38** (1999) 1113] [hep-th/9711200] [SPIRES].

[2] O. Aharony, S.S. Gubser, J.M. Maldacena, H. Ooguri and Y. Oz, *Large-N field theories, string theory and gravity*, *Phys. Rept.* **323** (2000) 183 [hep-th/9905111] [SPIRES].

[3] G. Policastro, D.T. Son and A.O. Starinets, *From AdS/CFT correspondence to hydrodynamics*, *JHEP* **09** (2002) 043 [hep-th/0205052] [SPIRES].

[4] D.T. Son and A.O. Starinets, *Minkowski-space correlators in AdS/CFT correspondence: Recipe and applications*, *JHEP* **09** (2002) 042 [hep-th/0205051] [SPIRES].

[5] D.T. Son and A.O. Starinets, *Viscosity, black holes and quantum field theory*, *Ann. Rev. Nucl. Part. Sci.* **57** (2007) 95 [arXiv:0704.0240] [SPIRES].

[6] A. Buchel, J.T. Liu and A.O. Starinets, *Coupling constant dependence of the shear viscosity in $N = 4$ supersymmetric Yang-Mills theory*, *Nucl. Phys.* **B 707** (2005) 56 [hep-th/0406264] [SPIRES].

[7] A. Buchel, *Resolving disagreement for eta/s in a CFT plasma at finite coupling*, *Nucl. Phys.* **B 803** (2008) 166 [arXiv:0805.2683] [SPIRES].

[8] Y. Kats and P. Petrov, *Effect of curvature squared corrections in AdS on the viscosity of the dual gauge theory*, *JHEP* **01** (2009) 044 [arXiv:0712.0743] [SPIRES].

[9] R.C. Myers, M.F. Paulos and A. Sinha, *Quantum corrections to eta/s*, *Phys. Rev.* **D 79** (2009) 041901 [arXiv:0806.2156] [SPIRES].

[10] A. Buchel, R.C. Myers, M.F. Paulos and A. Sinha, *Universal holographic hydrodynamics at finite coupling*, *Phys. Lett.* **B 669** (2008) 364 [arXiv:0808.1837] [SPIRES].

[11] A. Buchel, R.C. Myers and A. Sinha, *Beyond $\eta/s = 1/4\pi$*, *JHEP* **03** (2009) 084 [arXiv:0812.2521] [SPIRES].

[12] A. Sinha and R.C. Myers, *The viscosity bound in string theory*, *Nucl. Phys.* **A 830** (2009) 295c–298c [arXiv:0907.4798] [SPIRES].

[13] D.M. Hofman and J. Maldacena, *Conformal collider physics: Energy and charge correlations*, *JHEP* **05** (2008) 012 [arXiv:0803.1467] [SPIRES].

[14] D.M. Hofman, *Higher derivative gravity, causality and positivity of energy in a UV complete QFT*, *Nucl. Phys.* **B 823** (2009) 174 [arXiv:0907.1625] [SPIRES].

[15] M. Brigante, H. Liu, R.C. Myers, S. Shenker and S. Yaida, *The viscosity bound and causality violation*, *Phys. Rev. Lett.* **100** (2008) 191601 [arXiv:0802.3318] [SPIRES].

[16] M. Brigante, H. Liu, R.C. Myers, S. Shenker and S. Yaida, *Viscosity bound violation in higher derivative gravity*, *Phys. Rev.* **D 77** (2008) 126006 [arXiv:0712.0805] [SPIRES].

[17] A. Buchel and R.C. Myers, *Causality of holographic hydrodynamics*, *JHEP* **08** (2009) 016 [arXiv:0906.2922] [SPIRES].

[18] J. de Boer, M. Kulaxizi and A. Parnachev, *AdS_7/CFT_6, Gauss-Bonnet gravity and viscosity bound*, *JHEP* **03** (2010) 087 [arXiv:0910.5347] [SPIRES].

[19] X.O. Camanho and J.D. Edelstein, *Causality constraints in AdS/CFT from conformal collider physics and Gauss-Bonnet gravity*, *JHEP* **04** (2010) 007 [arXiv:0911.3160] [SPIRES].

JHEP08(2010)035

[20] A. Buchel et al., *Holographic GB gravity in arbitrary dimensions*, *JHEP* **03** (2010) 111 [arXiv:0911.4257] [SPIRES].

[21] X.-H. Ge and S.-J. Sin, *Shear viscosity, instability and the upper bound of the Gauss-Bonnet coupling constant*, *JHEP* **05** (2009) 051 [arXiv:0903.2527] [SPIRES].

[22] R.-G. Cai, Z.-Y. Nie and Y.-W. Sun, *Shear viscosity from effective couplings of gravitons*, *Phys. Rev.* **D 78** (2008) 126007 [arXiv:0811.1665] [SPIRES].

[23] R.-G. Cai, Z.-Y. Nie, N. Ohta and Y.-W. Sun, *Shear viscosity from Gauss-Bonnet gravity with a dilaton coupling*, *Phys. Rev.* **D 79** (2009) 066004 [arXiv:0901.1421] [SPIRES].

[24] M.J. Duff, *Observations on conformal anomalies*, *Nucl. Phys.* **B 125** (1977) 334 [SPIRES].

[25] S. Nojiri and S.D. Odintsov, *On the conformal anomaly from higher derivative gravity in AdS/CFT correspondence*, *Int. J. Mod. Phys.* **A 15** (2000) 413 [hep-th/9903033] [SPIRES].

[26] M. Blau, K.S. Narain and E. Gava, *On subleading contributions to the AdS/CFT trace anomaly*, *JHEP* **09** (1999) 018 [hep-th/9904179] [SPIRES].

[27] X.-H. Ge, S.-J. Sin, S.-F. Wu and G.-H. Yang, *Shear viscosity and instability from third order Lovelock gravity*, *Phys. Rev.* **D 80** (2009) 104019 [arXiv:0905.2675] [SPIRES].

[28] J. de Boer, M. Kulaxizi and A. Parnachev, *Holographic lovelock gravities and black holes*, *JHEP* **06** (2010) 008 [arXiv:0912.1877] [SPIRES].

[29] X.O. Camanho and J.D. Edelstein, *Causality in AdS/CFT and Lovelock theory*, *JHEP* **06** (2010) 099 [arXiv:0912.1944] [SPIRES].

[30] F.-W. Shu, *The quantum viscosity bound in lovelock gravity*, *Phys. Lett.* **B 685** (2010) 325 [arXiv:0910.0607] [SPIRES].

[31] R.C. Myers and A. Sinha, *Seeing a c-theorem with holography*, arXiv:1006.1263 [SPIRES].

[32] R.C. Myers and A. Sinha, *Anomalies, central charges and holography*, to appear.

[33] C. Imbimbo, A. Schwimmer, S. Theisen and S. Yankielowicz, *Diffeomorphisms and holographic anomalies*, *Class. Quant. Grav.* **17** (2000) 1129 [hep-th/9910267] [SPIRES].

[34] A. Schwimmer and S. Theisen, *Universal features of holographic anomalies*, *JHEP* **10** (2003) 001 [hep-th/0309064] [SPIRES].

[35] A. Schwimmer and S. Theisen, *Entanglement entropy, trace anomalies and holography*, *Nucl. Phys.* **B 801** (2008) 1 [arXiv:0802.1017] [SPIRES].

[36] R.C. Myers and B. Robinson, *Black Holes in Quasi-topological Gravity*, arXiv:1003.5357 [SPIRES].

[37] I. Fouxon, G. Betschart and J.D. Bekenstein, *The bound on viscosity and the generalized second law of thermodynamics*, *Phys. Rev.* **D 77** (2008) 024016 [arXiv:0710.1429] [SPIRES].

[38] H. Liu and A.A. Tseytlin, *$D = 4$ super Yang-Mills, $D = 5$ gauged supergravity and $D = 4$ conformal supergravity*, *Nucl. Phys.* **B 533** (1998) 88 [hep-th/9804083] [SPIRES].

[39] G. Arutyunov and S. Frolov, *Three-point Green function of the stress-energy tensor in the AdS/CFT correspondence*, *Phys. Rev.* **D 60** (1999) 026004 [hep-th/9901121] [SPIRES].

[40] A. Sinha, *On the new massive gravity and AdS/CFT*, *JHEP* **06** (2010) 061 [arXiv:1003.0683] [SPIRES].

JHEP08(2010)035

[41] I. Gullu, T.C. Sisman and B. Tekin, *Born-Infeld extension of new massive gravity*, *Class. Quant. Grav.* **27** (2010) 162001 [arXiv:1003.3935] [SPIRES].

[42] J. Oliva and S. Ray, *A new cubic theory of gravity in five dimensions: Black hole, Birkhoff's theorem and C-function*, arXiv:1003.4773 [SPIRES].

[43] J. Oliva and S. Ray, *A classification of six derivative lagrangians of gravity and static spherically symmetric solutions*, arXiv:1004.0737 [SPIRES].

[44] M. Henningson and K. Skenderis, *The holographic Weyl anomaly*, *JHEP* **07** (1998) 023 [hep-th/9806087] [SPIRES].

[45] M. Henningson and K. Skenderis, *Holography and the Weyl anomaly*, *Fortsch. Phys.* **48** (2000) 125 [hep-th/9812032] [SPIRES].

[46] V.K. Dobrev, E.K. Khristova, V.B. Petkova and D.B. Stamenov, *Conformal covariant operator product expansion of two spin 1/2 fields*, *Bulg. J. Phys.* **1** (1974) 42.

[47] V.K. Dobrev, G. Mack, V.B. Petkova, S.G. Petrova and I.T. Todorov, *Harmonic analysis on the N-dimensional Lorentz group and its application to conformal quantum field theory*, in *Lecture Notes in Physics* **63** (1977) 280 [SPIRES].

[48] I.T. Todorov, M.C. Mintchev and V.B. Petkova, *Conformal invariance in quantum field theory*, *Sc. Norm. Sup.*, Pisa Italy (1978), pg. 273 [SPIRES].

[49] H. Osborn and A.C. Petkou, *Implications of conformal invariance in field theories for general dimensions*, *Ann. Phys.* **231** (1994) 311 [hep-th/9307010] [SPIRES].

[50] D. Anselmi, M.T. Grisaru and A. Johansen, *A critical behaviour of anomalous currents, electric-magnetic universality and CFT_4*, *Nucl. Phys.* **B 491** (1997) 221 [hep-th/9601023] [SPIRES].

[51] N. Banerjee and S. Dutta, *Shear viscosity to entropy density ratio in six derivative gravity*, *JHEP* **07** (2009) 024 [arXiv:0903.3925] [SPIRES].

[52] J. Erdmenger and H. Osborn, *Conserved currents and the energy-momentum tensor in conformally invariant theories for general dimensions*, *Nucl. Phys.* **B 483** (1997) 431 [hep-th/9605009] [SPIRES].

[53] S.S. Gubser and I.R. Klebanov, *Absorption by branes and Schwinger terms in the world volume theory*, *Phys. Lett.* **B 413** (1997) 41 [hep-th/9708005] [SPIRES].

[54] .T. Horowitz and N. Itzhaki, *Black holes, shock waves and causality in the AdS/CFT correspondence*, *JHEP* **02** (1999) 010 [hep-th/9901012] [SPIRES].

[55] G.T. Horowitz and A.R. Steif, *Space-time singularities in string theory*, *Phys. Rev. Lett.* **64** (1990) 260 [SPIRES].

[56] J.I. Latorre and H. Osborn, *Modified weak energy condition for the energy momentum tensor in quantum field theory*, *Nucl. Phys.* **B 511** (1998) 737 [hep-th/9703196] [SPIRES].

[57] L. Brillouin, *Wave propagation and group velocity*, Academic Press (1960).

[58] R. Fox, C.G. Kuper and S.G. Lipson, *Faster-than-light group velocities and causality violation*, *Proc. Roy. Soc. Lond.* **A 316** (1970) 515.

[59] E. Krotscheck and W. Kundt, *Causality criteria*, *Commun. Math. Phys.* **60** (1978) 171.

[60] N. Iqbal and H. Liu, *Universality of the hydrodynamic limit in AdS/CFT and the membrane paradigm*, *Phys. Rev.* **D 79** (2009) 025023 [arXiv:0809.3808] [SPIRES].

JHEP08(2010)035

[61] N. Banerjee and S. Dutta, *Higher derivative corrections to shear viscosity from graviton's effective coupling*, *JHEP* **03** (2009) 116 [arXiv:0901.3848] [SPIRES].

[62] R.C. Myers, M.F. Paulos and A. Sinha, *Holographic hydrodynamics with a chemical potential*, *JHEP* **06** (2009) 006 [arXiv:0903.2834] [SPIRES].

[63] M.F. Paulos, *Transport coefficients, membrane couplings and universality at extremality*, *JHEP* **02** (2010) 067 [arXiv:0910.4602] [SPIRES].

[64] R.C. Myers, A.O. Starinets and R.M. Thomson, *Holographic spectral functions and diffusion constants for fundamental matter*, *JHEP* **11** (2007) 091 [arXiv:0706.0162] [SPIRES].

[65] R. Gregory and R. Laflamme, *Black strings and p-branes are unstable*, *Phys. Rev. Lett.* **70** (1993) 2837 [hep-th/9301052] [SPIRES].

[66] K.M. Case, *Singular potentials*, *Phys. Rev.* **80** (1950) 797.

[67] V. de Alfaro, S. Fubini and G. Furlan, *Conformal invariance in quantum mechanics*, *Nuovo Cim.* **A 34** (1976) 569 [SPIRES].

[68] S.R. Beane et al., *Singular potentials and limit cycles*, *Phys. Rev.* **A 64** (2001) 042103 [quant-ph/0010073] [SPIRES].

[69] L.D. Landau, E.M. Lifshitz, *Quantum mechanics: non-relativistic theory*, Pergamon Press (1977).

[70] M. Kulaxizi and A. Parnachev, *Supersymmetry constraints in holographic gravities*, arXiv:0912.4244 [SPIRES].

[71] T. Banks and A. Zaks, *On the phase structure of vector-like gauge theories with massless fermions*, *Nucl. Phys.* **B 196** (1982) 189 [SPIRES].

[72] F. Sannino, *Dynamical Stabilization of the Fermi scale: phase diagram of strongly coupled theories for (Minimal) walking technicolor and unparticles*, arXiv:0804.0182 [SPIRES].

[73] F. Sannino, *Phase Diagrams of Strongly Interacting Theories*, arXiv:1003.0289 [SPIRES].

[74] F. Sannino, *Conformal dynamics for TeV physics and cosmology*, arXiv:0911.0931 [SPIRES].

[75] E. Poppitz and M. Ünsal, *Conformality or confinement: (IR)relevance of topological excitations*, *JHEP* **09** (2009) 050 [arXiv:0906.5156] [SPIRES].

[76] E. Poppitz and M. Ünsal, *Conformality or confinement (II): one-flavor CFTs and mixed-representation QCD*, *JHEP* **12** (2009) 011 [arXiv:0910.1245] [SPIRES].

[77] U. Gürsoy and E. Kiritsis, *Exploring improved holographic theories for QCD: part I*, *JHEP* **02** (2008) 032 [arXiv:0707.1324] [SPIRES].

[78] U. Gürsoy, E. Kiritsis and F. Nitti, *Exploring improved holographic theories for QCD: part II*, *JHEP* **02** (2008) 019 [arXiv:0707.1349] [SPIRES].

[79] M. Jarvinen and F. Sannino, *Holographic conformal window - a bottom up approach*, *JHEP* **05** (2010) 041 [arXiv:0911.2462] [SPIRES].

[80] F. Bigazzi, R. Casero, A.L. Cotrone, E. Kiritsis and A. Paredes, *Non-critical holography and four-dimensional CFT's with fundamentals*, *JHEP* **10** (2005) 012 [hep-th/0505140] [SPIRES].

[81] R. Brustein and A.J.M. Medved, *The ratio of shear viscosity to entropy density in generalized theories of gravity*, *Phys. Rev.* **D 79** (2009) 021901 [arXiv:0808.3498] [SPIRES].

JHEP08(2010)035

[82] M. Paulos, *Lovelock theories, holography and the fate of the viscosity bound.*,unpublished.

[83] X.O. Camanho, J.D. Edelstein and M. Paulos, in preparation.

[84] D. Lovelock, *The Einstein tensor and its generalizations*, *J. Math. Phys.* **12** (1971) 498 [SPIRES].

[85] D. Lovelock, *Divergence-free tensorial concomitants*, *Aequationes Math.* **4** (1970) 127.

[86] G.T. Horowitz and R.C. Myers, *The AdS/CFT correspondence and a new positive energy conjecture for general relativity*, *Phys. Rev.* **D 59** (1998) 026005 [hep-th/9808079] [SPIRES].

[87] M. Henneaux, C. Teitelboim and J. Zanelli, *Quantum mechanics for multivalued Hamiltonians*, *Phys. Rev.* **A 36** (1987) 4417 [SPIRES].

[88] C. Teitelboim and J. Zanelli, *Dimensionally continued topological gravitation theory in Hamiltonian form*, *Class. Quantum Grav.* **4** (1987) L125.

[89] J. Alanen and K. Kajantie, *Thermodynamics of a field theory with infrared fixed point from gauge/gravity duality*, *Phys. Rev.* **D 81** (2010) 046003 [arXiv:0912.4128] [SPIRES].

[90] J. Alanen, K. Kajantie and K. Tuominen, *Thermodynamics of quasi conformal theories from gauge/gravity duality*, arXiv:1003.5499 [SPIRES].

JHEP08(2010)035